

International Journal of Automation and Safety



Editor-in-chief
Pr. Youcef ZENNIR

Co-editors
Pr. Fares INNAL
Pr. El-hadi GUECHI
Pr. Cherif TOLBA

Université 20 août 1955 Skikda-Algérie
BP 26 route El-hadeaik, 21000 Skikda, Algérie

Tel. : 00213664735277/ Fax. : 0021338723128
Email. : ijas@univ-skikda.dz

International Journal of Automation and Safety (IJAS)

Is an international peer-reviewed open-access journal
specialized in automation and Safety System.

Issued by the University of Skikda

Honorary President of the magazine:

Professor Pr. Toufik BOUFENDI

President of the University of Skikda

Editor-in-Chief: Professor Pr. Youcef ZENNIR - Institute of
Sciences and Techniques Applied- ISTA- University of Skikda

Issue: 00

International Journal of Automation and Safety (IJAS)

OBJECTIVES AND SCOPE OF JOURNAL

The International Journal of Automation and Safety IJAS is a comprehensive platform dedicated to advancing knowledge in the fields of automation science and safety science. Our aim is to provide a valuable resource for researchers, professionals, and students interested in the latest developments, theories, and applications in these areas.

This journal covers a wide range of topics related to automation and safety, including but not limited to industrial automation, robotics, artificial intelligence, control systems, risk and dependability assessment, hazard analysis, and safety management. By publishing high-quality research articles, reviews, and case studies, we aim to foster innovation, promote best practices, and contribute to the overall improvement of automation and safety practices. Multidisciplinary research that bridges the gap between automation and safety/reliability is particularly welcome.

Our editorial board comprises experts and scholars from academia, industry, and research institutions, ensuring the publication of cutting-edge and impactful research.

Whether you are an engineer, scientist, or professional working in automation or safety-related fields, the IJAS provides a platform to share and explore the latest advancements, emerging trends, and practical solutions. Join us in shaping the future of automation science and safety science.

IJAS is an international peer-reviewed open-access journal, disseminating the quality research in the following fields:

- Automation, systems and control,
- Autonomous systems,
- Multiagent systems,
- Decision-making and decision support,
- Robotics,
- Mechatronics,
- Data sciences,
- New computing paradigms,
- Principles and theory of risk assessment and management
- Risk assessment policy, standards and regulations
- Risk-based decision making and risk management
- Decision making and decision support systems for risk and disaster management on regional and global scales
- Risk perception and communications
- Risk assessment and control
- Risk characterisation
- Dynamic risk assessment

- Integration of risk models and quantifications
- Advanced concepts and information technologies in risk assessment and management
- Integrated risk assessment and safety management
- Integrated risk assessment in developing and rapidly developing countries, etc. Topics covered include.
- Diagnosis of continuous and discrete event systems (DES)
- Control of continuous, Discrete Event Systems and hybrid systems
- Fault-tolerant control
- Integrated modelling, simulation and analysis approaches for dependability assessment
- Dynamic reliability
- Process safety and environmental engineering
- Public health and medical services
- Process engineering and environmental protection
- Computer science and safety
- Health and safety at work
- Environmental and ecological systems
- Biology and human behavioral science

Editor in chief:

Pr. Youcef ZENNIR

Co-editors :

Pr. Fares INNAL

Pr. El-hadi GUECHI

Pr. Cherif TOLBA

Secretariat : Wahiba BOUCHARB

Scientific Committee:

Pr. Denis Pomorski (France)	Pr. Hamid Bentarzi (Algeria)	Dr. Amina Benaissa (Algeria)
Pr. Hichem Arioui (France)	Pr. Hacene Bouzakri (Algeria)	Pr. Abdelaziz Bouhadiba (Algeria)
Pr. Bernard Kamsu Fogoum (France)	Dr. Ghania Harzallah (Algeria)	Dr. Mohamed Rahim (Algeria)
Pr. Belkacem Old Boumama (France)	Pr. Abdelmajid Recioui (Algeria)	Pr. Youcef Soufi (Algeria)
Pr. Abdelouhab Aitouche (France)	Pr. Imad Ahriche (Algeria)	Dr. Yassine Bensafia (Algeria)
Dr. Paul Reaidy (France)	Pr. Lilia Zighed (Algeria)	Dr. Marsa Zoubida (Algeria)
Pr. Manuel Rodriguez (Spain)	Dr. Rochdi Bouchebbat (Algeria)	Dr. Bilal Zerouali (Algeria)
Pr. Saad Mekhilef (Malaysia)	Pr. Fayçal Arbaoui (Algeria)	Dr. Salima Lekhchine (Algeria)
Dr. Ammar Belatreche (UK)	Pr. Nabil Messikh (Algeria)	Pr. Khettab khatir (Algeria)
Dr. Olivier Pages (France)	Dr. Lamine Mehennaoui (Algeria)	Dr. Abdelhamid Djari (Algeria)
Pr. Horst Schulte (Germany)	Dr. Kamel Menighed (Algeria)	Pr. Mohamed Nemissi (Algeria)
Pr. Yiliu Liu (Norway)	Dr. Salima Ziani (Algeria)	Dr. Mohyiddine Hamaidia (Algeria)
Pr. Ahmed Rubaai (USA)	Dr. Salima Ait Ali (Algeria)	Dr. Zeroual Abdelhafid (Algeria)
Pr. Mary Ann Lundteigen (Norway)	Dr. Riad Bendib (Algeria)	Dr. Omeiri Hanane (Algeria)
Pr. Rochdi Merzouki (France)	Dr. El-Arkam Mechhoud (Algeria)	Dr. Bensaci chaima (Algeria)
Dr. Jesús Fernández Lozano, (Spain)	Pr. Smaine Mazouzi (Algeria)	Dr. Berghout Belkacem (Algeria)
Pr. Maan El Badaoui El Najjar (France)	Dr. Hichem Bounezour (Algeria)	Pr. Ridha Kelaiaia (Algeria)
Pr. Manuel Fernando dos Santos Silva (Portugal)	Pr. Nabil Bougdah (Algeria)	Pr. Azzedine Bouzaouit (Algeria)
Pr. Sebti Fofou (UAE)	Dr. Amira Otmani (Algeria)	Dr. Mohamed Boudiaf (Algeria)
Pr. Adam Belloum (Netherlands)	Pr. Salah Messast (Algeria)	Pr. Mohamed Salah Medjram (Algeria)
Pr. Vincent Cocquempot (France)	Pr. Samir Ladaci (Algeria)	Pr. Mounira Rouainia (Algeria)
Pr. Saso Blazic (Slovenia)	Pr. Fayçal Djazi (Algeria)	Dr. Nassira Ferroudj (Algeria)
Pr. Ahmed Chemori (France)	Pr. Ahcene Goutas (Algeria)	Pr. Mohamed Belkheiri (Algeria)
Pr. İlhami Colak (Turkey)	Pr. Aissa Belmeguenai (Algeria)	Pr. Emna Zouaoui (Algeria)
Pr. Şeref Sağıroğlu (Turkey)	Dr. Karim Baiche (Algeria)	Dr. Nesrine Ammouchi (Algeria)
Dr. Adel Merabet (Canada)	Dr. Saadia Saadi (Algeria)	Dr. Hedef Hefaidh (Algeria)

Dr. Samia Maza (France)	Dr. Belkhir Negrou (Algeria)	Dr.Fatiha Djemili (Algeria)
Dr. Jesus Enrique Sierra Garcia (Spain)	Pr. Abderrazak lachouri (Algeria)	Pr. Zahir Ahmida (Algeria)
Dr. Maher Kharrat (Tunisia)	Dr. Salah Bouhayene (Algeria)	Pr. Lotfi Messikh (Algeria)
Pr. Mohamed Chaabane (Tunisia)	Pr. Nadir Derouiche (Algeria)	Dr. Abderahmane Ganouche (Algeria)
Dr. Karim Chabir (Tunisia)	Dr. Khaoula Lassoued (Tunisia)	Dr. Nouara Ouazraoui (Algeria)
Dr. Fouzi Boulkenafet (Algeria)	Dr. Ibtissam Boussouf (Algeria)	Dr. Nadhir Abderrahmane (Algeria)
Dr. Bilel Ayachi (Algeria)	Pr. Hamid Boubertakh (Algeria)	Pr. Salim labiod (Algeria)
Pr. Noureddine Bessous (Algeria)	Dr. Faouzi Bouchareb (Algeria)	Dr. Nourreddine Nafir (Algeria)

Table of contents

<i>Article Title</i>	<i>author</i>	<i>pages</i>
Enhancing Urban Traffic Management through an Internet of Vehicles Framework	Somia Boubedra, Cherif Tolba	08
Optimal Placement and Sizing of Energy Storage Systems in Smart Grids	Abderrahmane Ouadi, Hamid Bentarzi	16
A new Algorithm for Image encryption based on chaotic systems	Djamel herbadji, Aïssa Belmeguenäi, Derouiche Nadir, Abderahmane herbadji	22
Based Security Control of Networked Control System under Communication Constraints	Nafir Nourreddine, Rouamel Mohamed, Bourahala Faycal	26
Studies and Analysis of the MPPT based DISMC of PV using Buck Converter connected to Battery	Yousra Izgheche, Tahar Bahi	32
Three-Dimensional Fuzzy Logic Controller Applied to Rocket Target Traction	F. Bourourou, I.Habi, S.A.Tadjer	36



Enhancing Urban Traffic Management through an Internet of Vehicles Framework

Somia Boubedra^{1*}, Cherif Tolba¹

¹ Computer Science Department, Badji Mokhtar University, Annaba, Algeria

Corresponding Author Email: as_boubedra@esi.dz

ABSTRACT

Received: 10/01/2023

Accepted: 21/06/2023

Published: 19/09/2023

Keywords:

Fog/Edge servers, Intelligent Transportation Systems (ITS), Internet of Things (IoT), Internet of Vehicles (IoV), Traffic Congestion, VANETs.

In recent years, the large number of vehicles has led to a considerable increase in urban traffic. As a result, road traffic has become one of the major problems in most major cities. Road traffic problems are congestions and accidents resulting huge loss of time, damage to property and environmental pollution. These issues explain why many research programs around the world aim to improve our transportation systems; this is indeed a difficult task because the distributed, open, dynamic and partially controllable nature of transport networks makes it a complex area. This paper deals with the problem of managing and monitoring an intelligent transportation system, especially the urban traffic system, the aim of our contribution is limiting the nuisance caused by the increase in the use of transport. Thus, better mobility means limiting the environmental impact of the pollution generated, and improving safety and conditions of people's life. In this paper, we provide a short review on the impact of integrating the Internet of Vehicles into intelligent transportation systems. Furthermore, we propose a network architecture-based Internet of Vehicles to efficiently manage and monitor urban traffic systems. Our proposition is based on several technologies, selected carefully, such as wireless sensor network, RFID radio identification technology, Fog/Edge computing, and Cloud Computing. Overall, the proposed architecture improves the coordination and the communication among the road network entities, leading to advanced transportation systems.

1. INTRODUCTION

In our daily lives, technology becomes an important aspect, as it plays a major role in all domains and offers great benefits to individuals and societies. This involves the exponential growth of the concept of the Internet of Things, which is the interconnection of billions of different types of devices and sensors, called "smart objects", so that they cooperate to meet our needs with restricted capacities in terms of energy, memory, and processing powers [1].

Moreover, Transportation systems have a strong impact on the development of our society. Effective movement of goods and people contributes to economic growth and changes our territories through a good accessibility. That is why the development in transportation is one of important factors to indicate the well-being of a country [2]. In addition, the use of New Information Technologies and Communications to improve the transportation systems become a central solution in the field. The increase in computing power and the great development

of the embedded systems, as well as the quality of sophisticated sensors, have made it possible to propose more effective control mechanisms; and better consideration of operators or users, the result is so-called Intelligent Transportation Systems (ITS).



Figure. 1 Intelligent Transportation System Model

However, the European report [3] on the evaluation of research programs in transport, Intelligent Transport Systems are considered vital for designing sustainable transport systems. According to this report, through the integration of information, communication and control technologies, ITS enable authorities, operators and individuals to make better decisions. ITS concern all systems that improve the use of means of transport using a set of technologies to meet the objectives of the domain.

Whatever the functionality associated with the ITS, it is built from data captured on the network, which is received and processed by software. As a result, all the advances in communications, sensors and computing are potentially benefiting the transportation systems. For example, the development of connected or autonomous vehicles is only possible through the implementation of communications between vehicles and with a suitable infrastructure, the deployment of high-performance sensors, and significant computing capabilities.

In addition, researchers of urban traffic systems have oriented their researches to the use of the Internet of Things' technologies, which led to the apparition of new concept: The Internet of Vehicles (IoV). IoVis based on the Internet, wireless sensor networks and sensing technologies to perform both intelligent recognition of road users (who are considered as objects), monitoring, and finally the management and the real-time treatment of road traffic.

To discuss the details of this topic, we have organized the rest of our paper as follows: In the next part, we provide a concise review of IoV, comparing it with VANETs, discussing its characteristics, and the different communication modes. After that, we propose an efficient IoV architecture, based on an IoV architecture, and we explain in detail its layers and its functioning.

Finally, we present the conclusion and the perspectives of this research work.

2. PROBLEM STATEMENT

The traffic flow in urban areas continues to be problematic and the number of fatalities and accidents on roadways remains high. It is assumed that the primary cause of road issues is human error. Therefore, it is necessary to reduce the amount of human involvement in the driving process. For that reason, automotive manufacturers have attempted to create car systems that assist drivers in safety and enhanced driving is necessary.

According to Ward's research, in 2010 they were more than 1 billion in operation worldwide, and total new vehicle sales suggest that there could be up to 2 billion vehicles by 2035. The traffic remains chaotic and the number of deaths and injuries on roadways remains high [4].

Moreover, more people live in urban areas than in rural areas, and cities are expected to continue growing. The United Nations estimates that in 2050 about 66 % of the

world's population would live in urban areas. Such development has a significant influence on the quality of human daily life [5].

Governments over the world have applied a variety of countermeasures in order to reduce road traffic accidents, such as laws to regulate road traffic, or automotive systems to help drivers in the driving process. Despite the wide variety of countermeasures applied by governments over the world, the transportation system still needs improvements [5].

Connected Vehicles, Intelligent Transportation Systems (ITS) along with IoT technologies, constitute the concept of the Internet of Vehicles and have the potential to release efficient and more sustainable transportation systems that are becoming increasingly important to people's daily lives [6].



Figure. 2 Traffic congestion in big cities.

3. GENERAL NOTIONS

2.1 Internet of Things (IoT)

In [7], IoT was defined as a "dynamic global network infrastructure with self-configuring capabilities based on standards and interoperable communication protocols; physical and virtual 'things' in an IoT have identities and attributes and are capable of using intelligent interfaces and being integrated as an information network".

From the viewpoint of network, the IoT is a very complicated heterogeneous network, which includes the connection between various types of networks through various communication technologies [8].

In addition, the Oxford Dictionaries offers a concise definition of the IoT: Internet of things (noun): The interconnection via the Internet of computing devices embedded in everyday objects, enabling them to send and receive data [9]

Furthermore, the capabilities offered by the IoT can save people and organizations time and money as well as help improve decision-making and outcomes in a wide range of application areas.[10]

As well, IoT plays an important role in transportation field, such, vehicles have increasingly powerful sensing, networking, and data processing capabilities For instance, IoT technologies make it possible to track each vehicle'

existing location, monitor its movement, and predict its future location. [8]

2.2 Internet Of vehicles (IoV)

It is a dynamic network, which consists of IoT enabled cars by using modern embedded and electronic devices like sensors and GPS, and integration of the information and communication systems to improve traffic flow, and to offer more effective road management and accident avoidance.

The urban traffic system has benefited from a lot of IoT applications like 'Internet of Vehicle' concept, Vehicle-to-Vehicle (V2V), and Vehicle to Infrastructure (V2I) communications, and have been transformed to a new level of interoperability, stability and efficiency, because, If vehicles communicate with each other, risks for accidents and mishaps would be very low. In addition, by using IoT technologies in the road traffic, we can monitor urban transportation systems, determine the state of traffic and pedestrian densities, identify damages and accidents, avoid collisions as needed, and optimize travel route [11].

4. IMPACTS OF TRAFFIC CONGESTION

Commonly, Traffic issues are a significant problem in urban areas, especially during rush hours [12]. According to [13] The United States spends over 836\$ billion on crash-related costs, insurance premiums, and traffic law enforcement. In addition, traffic congestion costs Americans 124\$ billion in direct and indirect losses, expected to reach 186\$ billion by 2030. Therefore, traffic congestion in urban areas can affect Road Users' quality of traveling, society, and the economy [12].

- **Road users:** Traffic jams in urban roads can cause stress to vehicle users. In addition to the waste of time for motorists and passengers as well as their productive abilities. Furthermore, it can reduce the precision of calculating travel for each road user.
- **Society:** Traffic congestion may increase fuel consumption, and as a result, it can lead to air pollution. Unfortunately, in some cases, the congestion in urban areas can be considered a direct reason for road accidents. On another societal side, it can create late delivery of goods.
- **Economy:** Bottlenecks in urban roads, and according to the previous impacts, may provoke a reduction in employees' performances. Which can cause a decrease in economic growth, and will force the government to spend on enhancing the Intelligent Traffic Management Systems.

5. INTERNET OF VEHICLES AND VANETS

The use of communication technology and smart devices in vehicles has revolutionized the automotive industry. As a result, intelligent transportation systems have emerged with vehicles equipped with sensors and computers that may collect and process data for information exchange [14]. Vehicular ad hoc networks (VANETs) were introduced to enable direct communication between

vehicles and infrastructure, but they face challenges such as unstable network services and limited handling of big data. In the era of 5G/B5G and the Internet of Things (IoT), VANETs are transforming into the Internet of Vehicles. Therefore, IoV aims to enhance safety, reduce congestion, and provide services through information exchange between vehicles and relevant entities. Moreover, IoV encompasses various communication models and relies on vehicle networking and intelligence technologies. These advancements expand the communication scope and potential of the IoV system [14].

5.1 Challenges in VANETS

The initial goals of VANET research technology were to ensure traffic safety [15], improve travel efficiency, and reduce pollutant emissions [16]. However, practical applications of VANET have faced challenges in commercialization. These challenges include the loss of network services when disconnected from other networks, incompatible network architectures, limitations in computing ability and storage space, and low accuracy of application services due to localized traffic data processing. To address these shortcomings, the emergence of the Internet of Vehicles offers promising prospects for the development of smart transportation systems. IoV overcomes the limitations of VANET through its heterogeneous network architecture, enabling cooperation with other communication networks. IoV is also compatible with most communication devices in daily life. The cooperation of different networks and the availability of multiple communication models (V2S, V2V, V2P, V2R, V2I) in IoV facilitate the sharing of big data, enhance the reliability of communication services, and expand the application scope of automotive communication. These advantages position IoV as a crucial development in the field [14].

5.2 Advantages of IoV

The Internet of Vehicles has attracted extensive attention from both academia and industry. It includes research areas such as intelligent transportation and telematics. The research focus of intelligent transportation is to improve travel efficiency and safety through projects such as the intelligent vehicle road system in the United States, the Eureka plan in Europe, and the advanced dynamic traffic information system in Japan. The Internet of Vehicles combines mobile Internet, intelligent transportation systems, cloud computing, automotive electronics, and geographic information system to become a mixture of Internet of Things (IoT) and mobile Internet applications in the field of transportation [17]. In [13], authors have cited several advantages of the IoV, in particular, we highlight the following ones:

- IoV has transformed the road network entities into "new mobile devices". Ex: Vehicles, pedestrians, drones, etc.
- IoV creates networks that support functions such as intelligent traffic management.

- IoV consists of inter-vehicular, intra-vehicular, and vehicular mobile Internet components, enabling continuous connectivity and information exchange in vehicles.
- IoV facilitates the exchange of information between vehicles, road infrastructures, passengers, drivers, sensors, roadside units, and the Internet.
- IoV enables various services such as traffic management, road safety, healthcare apps, comfort, and infotainment.
- Communication protocols and standards like IEEE 802.11p, DMAC, VC-MAC, AODV [18], [19], DSR, and GPRS, among others, are used in IoV.
- IoV differs from Intelligent Transportation Systems by emphasizing information exchange among vehicles, humans, and road infrastructures.
- Estimated benefits per vehicle per year include savings on insurance rates, operation costs, and time spent in traffic for vehicle users.
- Society benefits from decreased accidents, traffic jam control, and reduced CO2 emissions.
- IoV has the potential to create around 400,000 new jobs in the United States.
- The global market size for IoV components is estimated to reach 115.26 billion Euros by 2020, according to the European Union.

6. CHARACTERISTICS OF IOV

Furthermore, the Internet of Vehicles environments illustrates a multitude of significant characteristics that contribute to their unique nature and functionality. In particular, we highlight the following key aspects [20]:

- **Dynamic topology and non-uniform node distribution:** The IoV network is composed of various entities. One prominent characteristic of this network is the mobility of vehicles, pedestrians, cyclists, drones, and mobile radars, which are constantly changing their locations, speed, and direction. Furthermore, the distribution of these entities in an IoV network depends on several factors, such as road conditions and driving habits [20]. This mobility aspect requires efficient communication and coordination mechanisms to ensure seamless connectivity and accurate data exchange, even in high-speed scenarios.
- **Heterogeneity:** IoV encompasses diverse vehicles with different types of communication technologies, such as DSRC, 4G/LTE, WiFi, and Zigbee... The heterogeneous nature of IoV enables compatibility and interoperability between different vehicles and infrastructures [20].
- **Granularity:** In the IoV, vehicles on the road can be categorized into subsets called Sub-IoVs, which operate at a more localized level and have lower granularities. By using different granularities, the IoV enables flexible and scalable data collection and analysis for intelligent transportation systems [20].
- **Scalability:** The IoV network is massive, with a large number of vehicles and infrastructure; therefore,

IoV should be scalable rapidly, to handle the growing volume of data, the number of connected devices, and the complexity of IoV applications [20].

- **Big data and high processing capability:** In IoV networks, vehicles, sensors, road infrastructure, drivers, pedestrians, and all other entities continuously generate huge amounts of data. Therefore, it should be collected, aggregated, processed, and analyzed in real-time to make decisions and extract valuable insights for improving transportation efficiency [21]. Furthermore, data processing and decision-making are assured by the fog/edge servers for rapid responses and by the cloud servers for general and large-scale decisions.

6.2 Communication modes in IoV

The Internet of Vehicles is a considerable shift in vehicle networking, leading to the development of intelligent transportation systems. IoV is a heterogeneous network consisting of various communication modes illustrated in Figure 3:

- **Vehicle-to-Vehicle (V2V):** inter-vehicle communication allows vehicles on the road to exchange information, messages, and even sensor data. Such communication not only ensures road safety but also enables cooperative driving by sharing details like location, speed, acceleration, and destination of each vehicle.
- **Vehicle-to-Person (V2P):** it enables vehicles to communicate with drivers, pedestrians, cyclists, and traffic police personnel, providing them with important information to enhance safety and improve overall traffic management.
- **Vehicle-to-Roadside (V2R):** the exchange of information or messages between vehicles and roadside units, like traffic lights, road signs, toll booths, parking systems, cameras, and radars.
- **Vehicle-to-Infrastructure (V2I):** it represents the communication between vehicles and the infrastructure responsible for high processing capabilities via WiFi or cellular networks like LTE/4G/5G [14].
- **Vehicle-to-Sensors (V2S):** this communication enables vehicles to interact with various types of sensors located on both sides of the road such as radar sensors, Inductive Loop Detectors, Ultrasonic sensors, microwave sensors, infrared sensors, and acoustic sensors [22].

6.3 IoV application in transportation systems

The Internet of Vehicles has attracted widespread attention in the market and has applications in different fields of transportation, which can be divided into the following categories [20], [21], [23]:

- **Healthcare applications:** The main objective of this type of IoV application is to decrease road accidents, and as a consequence, road deaths, for instance: Intersection collision warning [21]. In addition to real-time communication between vehicles and healthcare professionals. In emergencies, vehicles equipped with

medical devices can establish a connection with doctors or specialists who can remotely provide guidance and instructions for immediate medical intervention. In addition, Vehicles can be equipped with sensors and wearable devices to monitor the health parameters of passengers or drivers.

- **Safety-related application:** Vehicles diagnostics and maintenance [21], hazardous location notification, and collision warning systems were designed to minimize the number of accidents in IoV networks.
- **Traffic efficiency application:** it offers enhanced route guidance and navigation, to improve road traffic management and advance the field of traffic routing, like in a previous research work [22].
- **Comfort-related applications:** smart parking systems [24] and energy supply stations.

7. METHODOLOGY

7.1 IoT Architectures' Background

In [25], authors surveyed existing IoT architectures, which are three-layer architecture, Middleware-based architecture, Service Oriented Architecture (SOA), and Five-layer architecture. Furthermore, they marked that the five-layer architecture is the most appropriate model for IoT applications, due to its simplicity, by the way, this later consists of five layers : 1. Objects layer or perception layer, which contains physical components like sensors, actuators, 2. Objects Abstraction layer, by using this layer we transfer data generated by Objects layer over WiFi, GSM... 3. Service management layer, which processes data, makes decisions, and delivers services over network protocols. 4. Application layer, that provides high quality smart services to meet customer's needs, and 5. The Business layer that supports decision-making based on big-data analysis.

Authors of [26] presented two types of IoT architectures; the basic Three-layer architecture, it consists of perception or sensor layer, Network layer and application layer, and the four-layer SoA-based IoT architecture, which is composed of Perception layer, Network layer, Service layer, and Application layer, service layer is made of service discovery, service composition, service management, and interfaces. According to the authors, the service-oriented architecture is more flexible and generic, because a service layer is developed between network layer and application layer to provide the data services in IoT architectures like data aggregation and processing in network layer, and data mining, data analytics in application layer. After that, they introduced the relevant enabling technologies and challenges of each layer, and they token the four-layer SoA-based IoT architecture as an example.

In [27], authors proposed a four-layer architecture for future heterogeneous IoT, which contains Sensing layer, Networking layer, Cloud computing, and Application layer, we explain each layer with more details in the next part of the paper.

7.2 The proposed IoV architecture

In [27], the authors propose a four-layer architecture for the future Internet of Things; we combine this architecture with the concept of fog/edge computing, and we add a novel layer to this architecture, which is the edge servers' layer. Then, we adapt this architecture to be destined for road traffic systems; in this section, we explain our architecture in more detail.

Layers of the proposed architecture

First, we present the layers of our architecture illustrated in Figure 3:

- **Sensing layer:** This layer represents the physical sensors, actuators, and RFID tags that aim to capture, collect, and transmit information [25]. A large number of sensors are deployed in the monitoring area [27], which is in our case the urban road; we use sensors to collect data about the state of the road (if it is congested, or there is an accident or a fire in the road). From vehicles that are equipped with RFID tags, and pedestrians who have all smart phones in their possession, or swatches connected to the internet. Those sensors send the captured data to the sink node, which we call the master node; we will explain its role in the Fog/Edge computing layer.

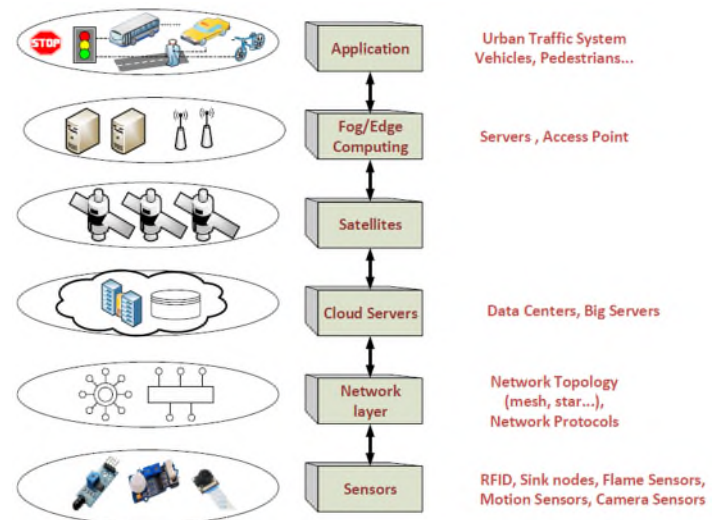


Figure 3: The proposed architecture's layers.

- **Network layer:** In this layer, we implement network protocols, and the corresponding topologies like star topology, tree topology, mesh topology, or hybrid topology, in order to forward data packets from source node to destination node [27]. However, we consider self-organizing network protocols, because we need more robustness and efficiency in the construction of network topology, like the IPv6 routing protocol "RPL", which is a distance vector routing protocol designed by the Internet Engineering Task Force IETF, for Low Power and Lossy Networks.
- **Cloud layer:** This layer is very important to handle the tremendous amount of data collected, and transmitted by other layers to cloud servers and big

data centers, to be processed, stored, and to make decisions based on data analysis [27], [26], thanks to the powerful analytical computing capacities that have cloud servers. Cloud computing is now a mature technology used to create, store, and use data over the Internet. Although, when a massive amount of data need to be stored, processed, and analyzed efficiently in data centers and cloud servers, a new technology appears to fulfill the gap, which is Fog/Edge computing, to extend cloud computing to be closer to the network of things [26].

- Satellite Sub-layer: To transmit data between Edge Servers and Cloud data centers and servers, we use Satellites, to gain time, throughput, and energy.
- Fog/Edge Computing layer: In this layer, we have two types of devices, the Master Nodes, and the Edge servers. We can use Edge servers for insuring processing, and storage and making decisions near the network, instead of doing all the computations in the cloud servers, hence, Edge computing has faster response and greater quality than cloud computing [26], especially, when we are faced to a real-time application like road traffic. We update data centers of the cloud once a day, at night, to minimize disruptions during peak hours, ensure that resources are available at night when fewer users are active, and reduce competition for bandwidth; on the other hand, we transmit data from master nodes to Edge Servers several times and periodically in the journey, because we can place some types of data for further computations and analysis, however, the high priority data, we address immediately to the closest Edge server, to ensure the real-time property of the road traffic system. The master node is an access point with good processing, energy, and transmission capacities, if we compare it with the road sensors, its role is to 1- receive the data collected by all the sensors near it, i.e. In the same area. 2- After that, it makes some calculations and data aggregations to reduce the big amount of the collected data, because and without a doubt, we will find a lot of redundancy, because, the sensors are in the same region and they will capture sometimes the same information.
- Application layer: The application layer responds to users' needs, by providing them the corresponding services [25], for instance, a car driver needs to know if this road is congested or not, he uses our application to get the best response. Our application here is urban road traffic management, which includes vehicles, pedestrians with their smartphones, or smart watches, road sensors, and other smart devices that are connected as objects in the network, delivered data is used to ensure the real-time management of the urban road traffic. Edge and cloud servers can manage and monitor remotely objects based on data analytics and visualization [27].

7.3 The functioning of the proposed architecture

Our Architecture is hybrid, in terms of connecting objects in the IoT network, which means that objects cooperate

with each other and exchange information on traffic; and hierarchical, because objects connect with the master node to transfer the data captured by sensors to the Edge Servers, in addition, data processing in edge servers will be sent for processing and make decisions to the cloud centers, as it's illustrated in Figure 4.

In each vehicle, we find a GPS (Global Positioning System); this later is responsible for receiving important data like location, time, and weather conditions from satellites [2]. In addition, we have RFID chips; their role is to exchange information with other vehicles and pedestrians and with road sensors using Zigbee IEEE 802.15.4. Road sensors are responsible for capturing road traffic data, from vehicles and pedestrians, these data tell us if there are congestions, accidents, or flames. . .

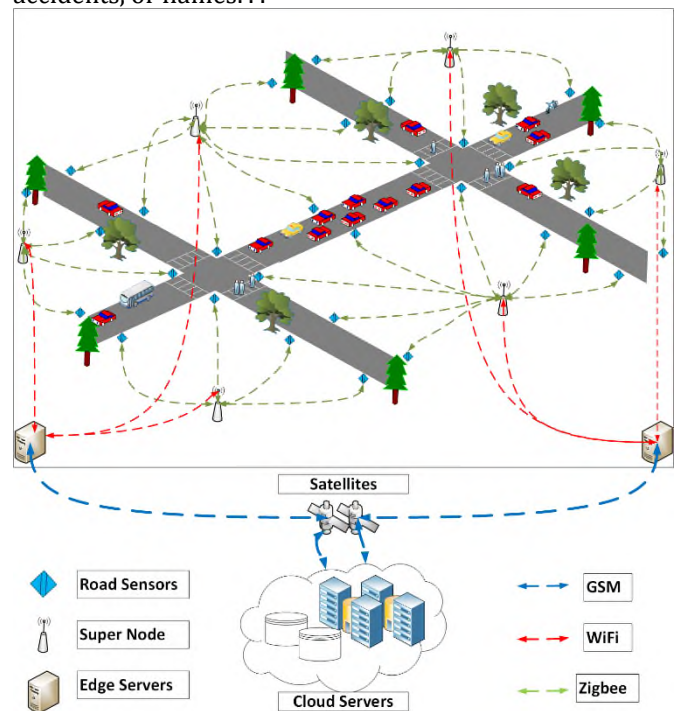


Figure.4: The proposed architecture of the ITS-based IoT

After that, they transmit the collecting data to the master node via WiFi IEEE 802.11. The master node consists of communication and data treatment modules; the communication part is a wireless antenna, which is responsible for receiving and decoding the transmitted data packets from the road sensors or the edge servers. Furthermore, the data treatment module is used to do some data aggregation on the data received from the road sensors, because there will be certainly redundancies, in addition, mechanisms of data aggregation aim to reduce the amount of transmission data and energy consumption [2]. The aggregated data are forwarded to the nearest edge server via GPRS (General Packet Radio Service), which is a cellular communication protocol, named 2.5 Generation (2.5 G), it means that is between the second generation and the third generation of GSM (Global System for Mobile communication). Each Edge Server make processing and calculations on data transmitted from Master nodes, make decisions, and preventions, to raise alarm to drivers or pedestrians to avert them if there is congestion, accidents,

and flames. . . to avoid more damage on the road; this process is repeating during all day long. Edge servers have a big power of storage and processing to make better decisions to ameliorate the quality of transportation in urban areas, they are an intermediary between Cloud servers and data centers, and sensor networks on the road. Processed data, decision-making, and preventions will be sent to Cloud servers through satellites, we use 4G to transfer data. Why use these existing protocols? We use any available network within the range, to insuring communication between components in an IoT system, which seems to be a better solution [2]. Like here

in our case, we use WiFi, and cellular networks like GPRS and 4G LTE, which are pre-existing network architectures, in order to avoid implementing new infrastructures. In Cloud centers, we make global and heavy operations, due to the big capacity of processing and storage, we use virtualization and data analytics to make better decisions and preventions and store data to use for improving the urban road traffic system.

CONCLUSIONS

The Internet of Vehicles is an important concept in the field of transportation and autonomous driving. It connects people, vehicles, and road infrastructure. It has gained commercial and economic interest and attracted the attention of researchers in the transportation area due to advancements in computation and communication technologies. This paper provides a short review of the impact of IoV on intelligent transportation systems by discussing problems and major issues in road systems, and the challenges in VANETS. After that, we present the key aspects of the IoV ecosystems: the most important characteristics, advantages, and modes of communication and the applications of IoV in transportation systems. Then, we present the IoV-based architecture. Therefore, the proposed architecture is generic and flexible for all urban traffic systems and can be applicable in the real world, because we bring together current and existing IoV and IoT technologies. The proposed architecture is global; we work to detail it more and more, using IoT and IoV technologies, and to implement its layers in the near future; once successfully implemented, the reduction of damages, collisions, congestion, and pollution in the urban road traffic will certainly benefit the quality of people's lives in urban areas.

REFERENCES

- [1] J. Subramaniam, L. H. Yean, and S. Manickam, "Intelligent IPv6 based IoT network monitoring and alerting system on Cooja framework," in *Journal of Fundamental and Applied Sciences*, vol. 9, pp. 661-670, 2017.
- [2] S. Vongsingthong, and S. Smanchat, "Internet of things- a review of applications & technologies", in *Suranaree Journal of Science and Technology*, vol. 21, no. 4, pp. 359-374, 2014.
- [3] "Innovate for a competitive and economical resources of transportation systems", Technical Report - European Union, 2012.
- [4] M. Alam, J. Ferreira, and J. Fonseca, "Introduction to intelligent transportation systems," *Intelligent transportation systems: Dependable vehicular communications for improved road safety*, pp. 1-17, 2016.
- [5] R. Silva, "Its-based decision making mechanism for opportunistic networking in heterogeneous network environment," Ph.D. dissertation, Ecole nationale sup'erieure Mines-T'el'ecom Atlantique Bretagne Pays de la Loire, 2020.
- [6] S. K. Datta, R. P. F. Da Costa, J. Harri, and C. Bonnet, "Integrating connected vehicles in internet of things ecosystems: Challenges and solutions," in *2016 IEEE 17th international symposium on a world of wireless, mobile and multimedia networks (WoWMoM)*. IEEE, 2016, pp. 1-6.
- [7] S. Li, L. D. Xu, and S. Zhao, "The internet of things: a survey", in *Information Systems Frontiers*, vol. 17, no. 2, pp. 243-259, 2015.
- [8] L. D. Xu, W. He, and S. Li, "Internet of Things in Industries: A Survey", in *IEEE Transactions on Industrial Informatics*, vol. 10, no. 4, pp. 2233-2243, 2014.
- [9] K. Rose, S. Eldridge, L. Chapin, "The Internet of Things: An Overview - Understanding the Issues and Challenges of a More Connected World", Internet Society, 2015.
- [10] A. Whitmore, A. Agarwal, and L. D. Xu, "The Internet of Things - A survey of topics and trends", in *Information Systems Frontiers*, vol. 17, no. 2, pp. 261-274, 2015.
- [11] P. Suresh, V. Daniel, V. Parthasarathy, R.H. Aswathy, "A state of the art review on the Internet of Things (IoT), History, Technology and fields of deployment", in *International Conference on Science, Engineering and Management Research (ICSEMR 2014)*, Chennai, India, 2014.
- [12] M. A. Zamri and N. Hamzah, "The implementation of intelligent traffic management system in solving traffic congestion: A survey of federal route 3214," in *Journal of Physics: Conference Series*, vol. 2319, no. 1. IOP Publishing, 2022, p. 012032.
- [13] J. Contreras-Castillo, S. Zeadally, and J. A. Guerrero-Ibanez, "Internet of vehicles: architecture, protocols, and security," *IEEE internet of things Journal*, vol. 5, no. 5, pp. 3701-3709, 2017.
- [14] B. Ji, X. Zhang, S. Mumtaz, C. Han, C. Li, H. Wen, and D. Wang, "Survey on the internet of vehicles: Network architectures and applications," *IEEE Communications Standards Magazine*, vol. 4, no. 1, pp. 34-41, 2020.
- [15] D. Bektache, C. Tolba, and N. Ghoualmi-Zine, "Forecasting approach in vanet based on vehicle kinematics for road safety," *International Journal of Vehicle Safety*, vol. 7, no. 2, pp. 147-167, 2014.
- [16] H. Brahmia and C. Tolba, "Nakagami fading impact on the performances of vanet routing protocols in a realistic urban area setting," *International Journal of*

- Advanced Networking and Applications, vol. 11, no. 4, pp. 4330–4335, 2020.
- [17] F. Yang, J. Li, T. Lei, and S. Wang, “Architecture and key technologies for internet of vehicles: a survey,” *Journal of communications and information networks*, vol. 2, no. 2, pp. 1–17, 2017.
- [18] H. Brahmia and C. Tolba, “Vanet routing protocols: discussion of various ad-hoc on-demand distance vector (aodv) improvements,” in *2018 3rd International Conference on Pattern Analysis and Intelligent Systems (PAIS)*, 2018, pp. 1–6.
- [19] F. Djemili and C. Tolba, “A mixed approach load balancing and efficient energy for multi-path routing in mobile ad hoc networks,” in *SENSORS*, 2013 IEEE, 2013, pp. 1–4.
- [20] S. Sharma and B. Kaushik, “A comprehensive review of nature-inspired algorithms for internet of vehicles,” in *2020 International Conference on Emerging Smart Computing and Informatics (ESCI)*. IEEE, 2020, pp. 336–340.
- [21] “A survey on internet of vehicles: Applications, security issues solutions,” *Vehicular Communications*, vol. 20, p. 100182, 2019.
- [22] S. Boubedra, C. Tolba, P. Manzoni, D. Beddiar, and Y. Zennir, “Urban traffic flow management on large scale using an improved aco for a road transportation system,” *International Journal of Intelligent Computing and Cybernetics*, vol. ahead-of-print, no. ahead-of-print, 2023.
- [23] M. Karoui, “Congestion mitigation and network selection management in a heterogeneous c-its communication architecture,” Ph.D. dissertation, Université Clermont Auvergne, 2021.
- [24] K. Rasheed, L. Shahzad, S. Saad, H. A. Khan, W. Ahmed, and T. Sadiq, “Parking guidance system using wireless sensor networks,” in *2021 International Conference on Decision Aid Sciences and Application (DASA)*, 2021, pp. 573–577.
- [25] A. Al-Fuqaha, M. Guizani, M. Mohammadi, M. Aledhari, and M. Ayyash, “Internet of Things: A Survey on Enabling Technologies, Protocols, and Applications”, in *IEEE Communication Surveys & Tutorials*, vol. 17, no. 4, pp. 2347-2376, 2015.
- [26] J. Lin, W. Yu, N. Zhang, X. Yang, H. Zhang, and W. Zhao, “A Survey on Internet of Things: Architecture, Enabling Technologies, Security and Privacy, and Applications”, in *IEEE Internet of Things Journal*, vol. 4, no. 5, pp. 1125-1142, 2017.
- [27] T. Qiu, N. Chen, K. Li, M. Atiquzzaman, W. Zhao, “How Can Heterogeneous Internet of Things Build our Future: A Survey”, in *IEEE Communications Surveys and Tutorials*, vol. 20, no. 3, pp. 2011-2027, 2018.



Optimal Placement and Sizing of Energy Storage Systems in Smart Grids

Abderrahmane Ouadi^{1*}, Hamid Bentarzi¹

¹Laboratory Signals and system, IGEE, University M'hamed Bougara Boumerdes

Corresponding Author Email: a.ouadi@univ-boumerdes.dz

ABSTRACT

Received: 20/02/2023

Accepted: 21/07/2023

Published: 19/09/2023

Keywords:

Voltage instability, Static Var Compensator (SVC), IEEE 9-bus power network

In recent years, numerous incidents of voltage instability have occurred in smart power grids. The primary factor contributing to this instability is the reactive power limit of the system. Flexible Alternating Current Transmission Systems (FACTS) devices can play a pivotal role in mitigating voltage instability. One such FACTS device is the Static Var Compensator (SVC), which offers significant and continuous voltage control across various operational conditions. In this context, this paper introduces a novel algorithm designed to determine the optimal placement and sizing of Static Var Compensators, aiming to enhance the voltage security of power systems during substantial disturbances. The selection of the most suitable location and appropriate size for the SVC is based on the sensitivity of the voltage magnitude, specifically dV/dQ . To validate the effectiveness of this approach, simulations were conducted using a model of an IEEE 9-bus power network. The purpose was to showcase the positive outcomes resulting from well-implemented SVCs.

1. INTRODUCTION

The power system is undergoing a transformation towards a more decentralized and intelligent power grid. This transition involves increased adoption of distributed generation and active participation of end-users. It is widely recognized that the demand for flexibility is growing. Even conventional power generation methods, which have been in use for decades, are grappling with rising power consumption demands. As a consequence, stability is diminishing, particularly in terms of reactive power within the system.

In this context, the concept of flexibility has been defined diversely. One such definition characterizes it as the alteration of generation injection and/or consumption patterns, either at an individual or collective level. This modification is often triggered by external signals and aims to serve the energy system or uphold stable grid operations [1]. In scenarios where voltage limits need to be maintained, reactive power is injected locally. However, unlike active power, reactive power cannot be transmitted over long distances, necessitating its local provision through various means [2].

Therefore, Flexible Alternating Current Transmission System (FACTS) controllers emerge as a fitting solution to supply reactive power locally. While generators possess reactive power control capabilities, the location of reactive power demand can significantly limit their effectiveness. Given the substantial costs associated with FACTS devices,

their optimal placement within the system is crucial. The impacts of Thyristor-Controlled Series Capacitors (TCSC) and Static Var Compensators (SVC) on system load curtailments are studied by placing these devices within the system using a trial-and-error approach. However, relying on a trial-and-error methodology lacks a rigorous mathematical foundation for determining the best location of these controllers. As these devices involve considerable expenses, a more systematic mathematical method is proposed in this study. SVC is chosen for this purpose due to its cost-effectiveness.

This work demonstrates how the application of FACTS technologies, such as SVC, serves as an effective solution for addressing instability issues. It helps prevent voltage collapse and enhances the overall stability of the power system.

2. STATIC VAR COMPENSATOR

The establishment of a Smart Grid necessitates advanced technologies to optimize its functionality and intelligence. The term "Smart Grid" should be perceived as an opportunity to enhance power system performance and elevate operational capabilities. Among the devices contributing to this enhancement are Flexible Alternating Current Transmission System (FACTS) devices, with the Static Var Compensator (SVC) standing out as a significant technology for power system compensation. SVC operates as a control device, offering rapid response times that

outpace traditional mechanically switched reactors or capacitors.

2.1 System Modeling

SVC serves as a shunt-connected variable generator or absorber. Its output is adjusted to exchange capacitive or inductive current, which in turn maintains or controls specific parameters of the electric power system, often focusing on bus voltage regulation. This device incorporates distinct components for generating leading and lagging Vars [3].

Within the active control range, the susceptance (B_{svc}) and the associated reactive current can be adjusted based on the voltage regulation slope characteristics illustrated in Figure 1. The specific slope value hinges on factors such as desired voltage regulation, allocation of reactive power among different sources, and additional system requirements. Typically, this slope value ranges from 1% to 5%. The behavior of the SVC is akin to a shunt capacitor set to its maximum value (B_{Cmax}) when operating at the capacitive limit. Conversely, it functions as a fixed shunt reactor at the minimum value ($-B_{Lsvc}$) when approaching the inductive limit. These limits become relevant during substantial fluctuations in bus voltage. The inductive limit becomes applicable as the bus voltage surpasses the upper threshold, while the capacitive limit comes into play when the voltage falls below the lower limit [4].

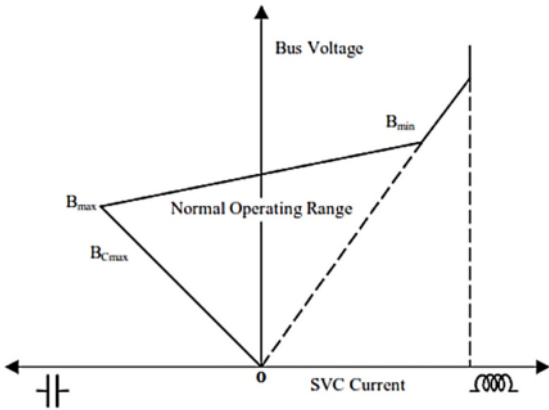


Figure. 1 SVC output characteristics.

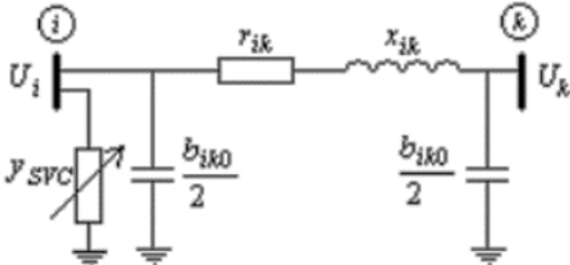


Figure. 2 Equivalent circuit of an SVC connected to a bus terminal.

Generally, the shunt connected SVC can be represented by its shunt current injection model. The current injection (I_{svc}) into the bus, where the SVC is connected, can be written as

$$I_{svc} = jB_{svc}V \quad (1)$$

$$B_{svc} = B_c - B_{TCR} = \frac{1}{X_c X_l} \left\{ X_l - \frac{X_c}{\pi} [2(\pi - \alpha) + \sin 2\alpha] \right\},$$

$$X_L = \omega L, X_c = \frac{1}{\omega C} \quad (2)$$

Where, B_{svc} , α , X_L , X_c are the shunt susceptance, firing angle, inductive reactance, and capacitive reactance of the SVC, respectively. $\omega = 2\pi f$, where f is the frequency of the supply.

The reactive power injected into the bus due to SVC can be expressed as:

$$Q_{svc} = B_{svc} V^2 \quad (3)$$

Where V is the voltage magnitude of the bus at which the SVC is connected.

The SVC can be modeled by a shunt variable admittance and can be placed either at the terminal bus of a transmission line or in the middle of a long line [5]. Considering the SVC without losses, the admittance only has its imaginary component and it can take values in a specified range (usually between 0 and the maximum SVC capacity studied). This is denoted by:

$$y_{svc} = jb_{svc} \quad (4)$$

This part considers the case of an SVC installed in a node Fig.3 with a continuously variable set point [6].

In this case, only one term of the nodal admittances matrix is modified, corresponding to the node where the SVC is connected:

$$Y_{ii}' = Y_{ii} + y_{svc} \quad (5)$$

The matrix is therefore modified as follows:

$$[Y'_{nn}] = \begin{bmatrix} y_{-ik} + \frac{y_{ik0}}{2} + y_{svc} & -y_{ik} \\ -y_{ik} & y_{-ik} + \frac{y_{ik0}}{2} \end{bmatrix} \quad (6)$$

3. PROBLEM FORMULATION

Consider a transmission network represented by its nodal admittance matrix $[Y_{nn}]$ and the vector of nodal powers $[S]$. Let S_v be the vector of state variables (voltage phase and magnitude) and let C_v be the set of control variables (location, size, reference SVC values, the domain of variable location – consisting in a set of nodes where the SVC placement study is carried out).

The problem lays in determining S_v and C_v to minimize or maximize a certain objective function $f(S_v, C_v)$ while verifying the following two types of constraints:

$$g(S_v, C_v) = 0 \text{ (Kirchhoff's law)}$$

$$h(S_v, C_v) \leq 0 \text{ (security constraints)} \quad (7)$$

The domains of definition for the variables are also set as inequality constraints.

The objective function when searching for optimal SVC locations can include several optimization criteria. This work proposes a multi-objective function, searching for a solution consisting of both the SVC location and SVC size that minimizes the voltage deviations, active power losses, and installation costs.

The objective function consists of three objectives, two of which are technical and one economical, as follows:

A. Minimize the active power losses:

$$O_1 = \sum_{l=1}^b R_l I_l^2 = \sum_{l=1}^b [V_l^2 + V_j^2 - 2V_l V_j \cos(\delta_i - \delta_j)] Y_{ij} \cos \varphi_{ij} \quad (8)$$

where b is the number of branches, R_l is the resistance of line l, I_l is the current through line l, V_i are the voltage magnitude and angle from node i and Y_{ij}, φ_{ij} are the magnitude and angle of the i-j line admittance

B. Minimize the voltage deviations

$$O_2 = \sum_{i=1}^n \left(\frac{U_{iref} - U_i}{U_{iref}} \right)^2 \quad (9)$$

Where n is the number of buses, U_{iref} is the reference voltage at bus i and U_i is the actual voltage at bus i.

Operational constraints

Power flow balance equations. The balance of active and reactive powers must be satisfied in each node:

$$P_{Gi} - P_{Li} = U_i \sum_{k=1}^n [U_k [G'_{ik} \cos(\theta_i - \theta_k) + B'_{ik} \sin(\theta_i - \theta_k)]]$$

$$Q_{Gi} - Q_{Li} = U_i \sum_{k=1}^n [U_k [G'_{ik} \sin(\theta_i - \theta_k) + B'_{ik} \cos(\theta_i - \theta_k)]] \quad (10)$$

where the conductance G'_{ik} and susceptance B'_{ik} represent the real and imaginary components of element Y'_{ik} of the [Y'_{nn}] matrix, obtained by modifying the initial nodal admittance matrix when introducing the SVC.

Power flow limits.

The apparent power that is transmitted through a branch I must not exceed a limit value, S_{lmax}, which represents the thermal limit of the line or transformer in steady-state operation:

$$S_l \leq S_{lmax} \quad (11)$$

Bus voltages.

For several reasons (stability, power, and quality, etc.), the bus voltages must be maintained around the nominal value:

$$V_{imin} \leq V_{inom} \leq V_{imax} \quad (12)$$

In practice, the accepted deviations can reach up to 10% of the nominal values.

SVC reference value

The size of an SVC is expressed as an amount of reactive power connected to a bus of voltage 1p.u. Sign conventions: a positive value indicates the fact that the SVC generates reactive power and injects it into the network through the node to which it is connected (capacitive state); a negative value characterizes the inductive state, where the SVC absorbs reactive power from the network.

The SVC size is a variable that can take nv discrete values from the interval:

$$Q_{Lmax} < Q_{svc} < Q_{Cmax} \quad (13)$$

The SVC in our case will be modeled as a reactive power generator connected to a bus in a system .

The reactive power generated by SVC is given by:

$$Q_{SVC}^{Min} \leq Q_{SVC} \leq Q_{SVC}^{Max} \quad (14)$$

If the SVC is operating outside the limits, so the bus becomes PQ-type and the reactive power Q is set and is expressed by

$$Q = -B * V^2 \quad (15)$$

Where

B: equivalent susceptance of the SVC

V: the calculated voltage magnitude at the SVC node.

4. PROPOSED ALGORITHM

In this work, the main objective is to find the optimal location and determine the size of the SVC for enhancing voltage security during emergency operating conditions.

This can be achieved through minimizing the sensitivity of voltage magnitude (dV/dQ) under severe line contingencies. The objective function is given by:

$$F_1 = \text{Minimize}[F] \quad (16)$$

The term F represents the dynamic voltage deviation (dV/dQ) at each node. The minimum value of the sensitivity of voltage magnitude (dV/dQ) is used to find the best location of SVC. Dynamic voltage deviation is calculated as follows:

$$F = \sum_{k=1}^{N_{PQ}} \frac{(V_i - V_{up})}{(Q - Q_0)} \quad (17)$$

Where: V_i is the voltage magnitude at node i.

V_{up} is the upper limit of the voltage at node i.

V_{low} is the lower limit of the voltage at node i.

The equality and inequality constraints are:

-Load Flow:

$$Q_{Gi} - Q_{Di} - \sum_{j=1}^N V_i V_j Y_{ij} \sin(\delta_{ij} + \gamma_j - \gamma_i) = 0 \quad (18)$$

$$P_{Gi} - P_{Di} - \sum_{j=1}^N V_i V_j Y_{ij} \cos(\delta_{ij} + \gamma_j - \gamma_i) = 0 \quad (19)$$

-Reactive Power of SVCs:

$$Q_i^{min} \leq Q_i \leq Q_i^{max} \quad (20)$$

Where Q_i is reactive power injection at node i by SVC;

-Voltage

$$V_i^{min} \leq V_i \leq V_i^{max}; i \in N_{Node} \quad (21)$$

Where V_{imin} and V_{imax} are minimum and maximum voltage at node i respectively.

Optimal placements of SVC controllers

The proposed algorithm for finding the optimal placement of SVC controllers involves the following steps:

- Create several critical contingencies such as line outage or generator outage. Then, load flow computation is done, and voltage magnitudes of several 220 kV nodes are computed for each contingency.

-Once the voltage magnitudes enter the specified dynamic limits (V_{lower} < V_i < V_{upper}), the voltage sensitivity dv/dq is computed for each contingency.

-The process is continued until the voltage magnitudes are less than the lower limit of the voltage at node i Then, nodes are ranked according to the dv/dq values.

The flowchart of the proposed algorithm is shown in Figure 3.

This paper proposes a new algorithm to find the optimal location and size of SVC controllers in order to increase the voltage security of power systems during large disturbances. The optimal location and size of SVC are determined based on the voltage magnitude sensitivity factor.

5. SIMULATION RESULTS AND DISCUSSION

For the testing and evaluation of the proposed algorithm, the test set up system IEEE 9 bus model is considered. The IEEE 9 bus system that is illustrated in Figure 4 consists of 3 generating units and 9 buses out of which one is the swing bus [7]. Four cases are studied taking into consideration the load bus voltages profiles for each case.

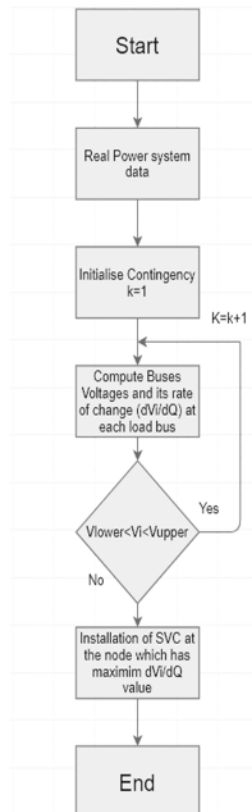


Figure. 3 Flowchart of the proposed algorithm.

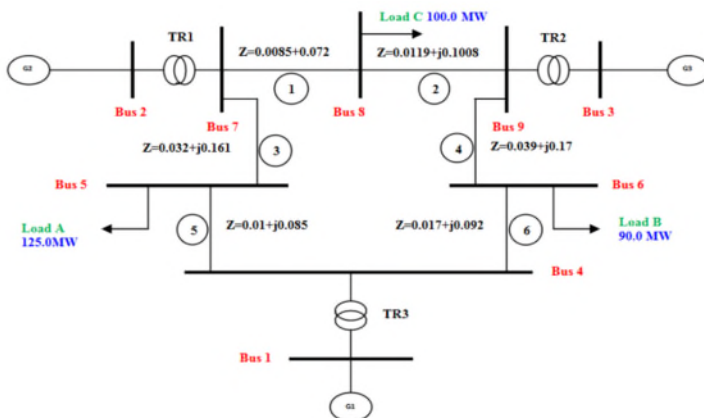


Figure. 4 IEEE 9 Bus Power Network Model.

The PSS@E software has been used for simulating the dynamic of the disturbance and presenting the frequency generators and load bus voltages plots before and after the implementation of the load shedding scheme. After simulating the proposed algorithm using PSS@E software, Matlab has been used to determine the main parameters of the algorithm which are the bus where the maximum value of dV/dQ can be obtained and the size of SVC. The simulation is done by considering the following cases.

Scenario 1: Loss of Transmission Line 3

The case study 1 of the IEEE 9 bus system considers the loss of transmission line 3 connecting bus 5 to bus 7. The resulting load bus voltages waveforms obtained from PSSE during the disturbance without installing SVC are shown in the figure 5.

The most critical lines of the IEEE 9 bus model are the lines that are connecting the generator buses to the remaining buses of the system. If a generator has only one transmission line connecting to the power system, this becomes a crucial line as its loss can result in the isolation of the generator from the whole system which is equivalent to the studies that will be carried out in the next case studies.

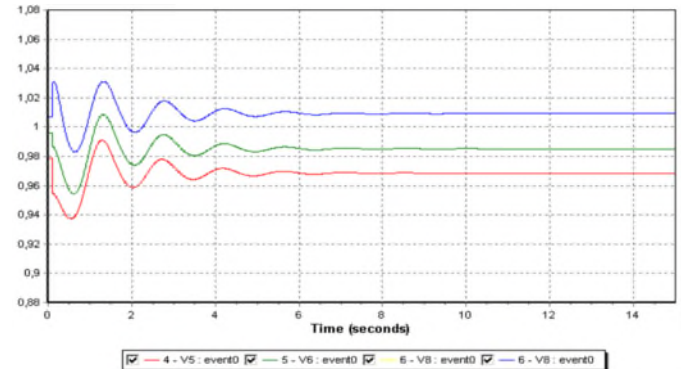


Figure. 5 Case 1 : Load Bus voltages (without SVC).

In this case, tripping the line 3 is not really crucial since we still have line 1 that is connecting generator 2 to the power system. As a result, the load bus voltages are not really affected much by this disturbance. This latter is considered as a very small disturbance that does not require any compensation. However, the recovery of the very small decline of the system load bus voltages is done by the spinning reserve.

Scenario 2: Outage of Generator 3

The case study 2 that we considered for the IEEE 9 bus model is the loss of generator 3. This causes the load bus voltages to be reduced after the disturbance takes place and before installing any SVC, the load bus voltages behaviors are shown in the figure 6.

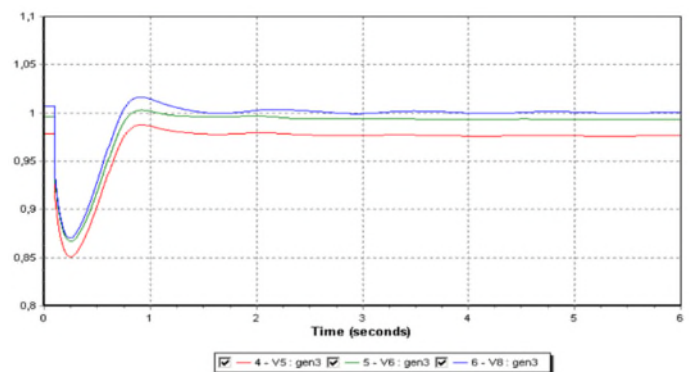


Figure. 6 Case 2: Load Bus Voltages before installing SVC

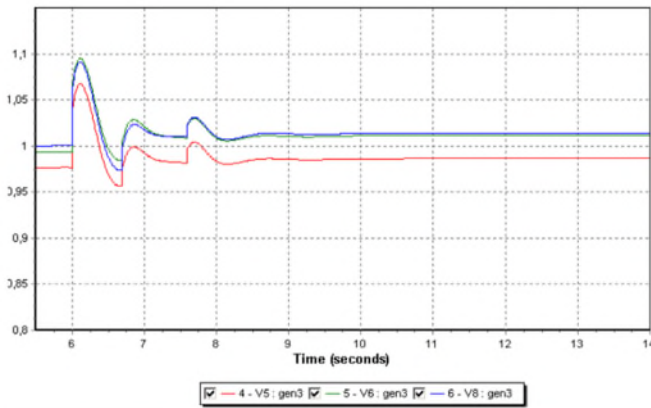


Figure. 7 Case 2: Load Bus Voltages after installing SVC

Figure 6 represents the load bus voltages before installing SVC. These voltages decrease below the rated value and they become stable at the following values:

- Voltage at load Bus 5: 0.976 p.u,
- Voltage at load Bus 6: 0.99 p.u,
- Voltage at load Bus 8: 1.00 p.u

Now, the voltage sensitivities for each load bus under this case are given in table 1.

Table I Voltage Sensitivities at each Load Bus (Case Study 2)

Load bus Number	dV/dQ
5	0.000103188
6	0.000479844
8	0.000193001

The maximum value of dV/dQ value is 0.000479844 at bus 6. It can be noticed that the SVC with a range between 100 Mvar and 200 Mvar to be installed at any load bus gives good results. The load bus voltages experience a gradual improvement. This can be noticed in Fig.7.

Scenario 3: Outage of Generator 3 with increase of load A & C by 50 %

The third case study of the IEEE 9 bus system considers the loss of a generator at bus 3 with an increase of load A & C by 50 %. This loss caused a reduction in the total generated power of the system by 196.6885 MW. The load bus voltages are also affected by the loss in the generated power. This can be seen in the plots of the load bus voltages in figure 8.

Before installing SVC, the load bus voltages decrease below their predetermined standards and become stable at the following lower values: -Voltage at load Bus 5: 0.95477 p.u,

-Voltage at load Bus 6: 0.97328 p.u, - Voltage at load Bus 8: 0.98175 p.u.

The voltage sensitivities; dV/dQ values are calculated individually for each load bus and the results are listed in table 2.

Table II Voltage Sensitivities at each Load Bus (Case Study 3)

Load bus number	dV/dQ
5	0.000926756
6	0.000103185
8	0.000850300

The maximum value of the dV/dQ is 0.000926756. The SVC with a range between 100 Mvar and 200 Mvar to be installed at each load bus is obtained using the voltage sensitivity with maximum value according to the proposed algorithm. It can be noticed that the best results can be obtained when the SVC of 130 Mvar is installed at bus 5. The load bus voltages experience a gradual improvement. This can be noticed in Fig.9.

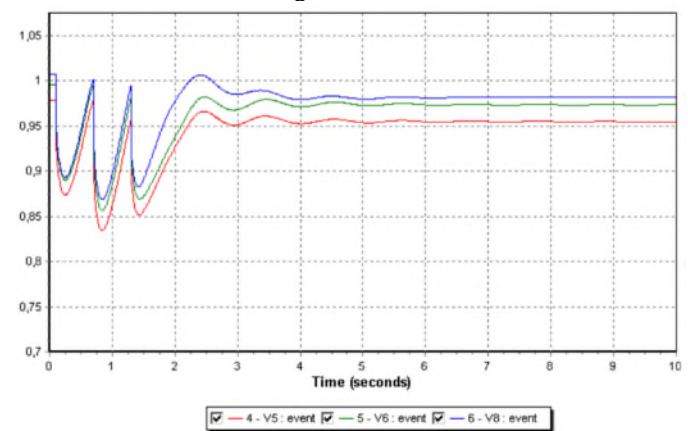


Figure. 8 Case 3: Load Bus Voltages before SVC installation.

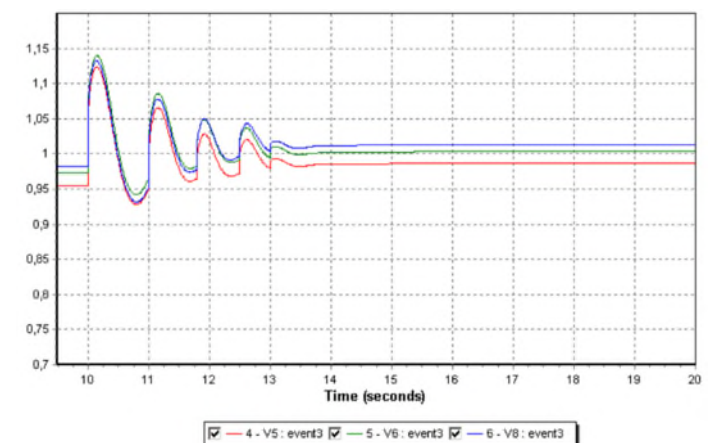


Figure. 9 Case 3: Load Bus Voltages after SVC installation.

Scenario 4: Increase of Load A, B & C by 100 % (Overload)

The last case study of the IEEE 9 bus system is the overload that consists in an increase of load A, B & C by 100 %. The generation power loss due to this overload is 314.6885 MW. The load bus voltages plots after the disturbance and before installing SVC are illustrated in Figures 10 and 11.

The load bus voltages are also changed due to the loss of some of the generated power. As it can be seen in the figure above. The load bus voltages are definitely lower than the acceptable values such as: -Voltage at load Bus 5: 0.924 p.u., -Voltage at load Bus 6: 0.926 p.u, and -Voltage at load Bus 8: 0.9761 p.u.

Table IV Voltage Sensitivities at each Load Bus (Case Study 4)

Load bus number	dV/dQ
5	0.001194300
6	0.000859908
8	0.000955450

The voltage sensitivities for this case are calculated and tabulated in table 3. The maximum value of the dV/dQ is 0.0011943. After installing SVC with 190 MVar at bus 5 according to our proposed algorithm, the voltage profile has been improved very much; as shown in figure 11.

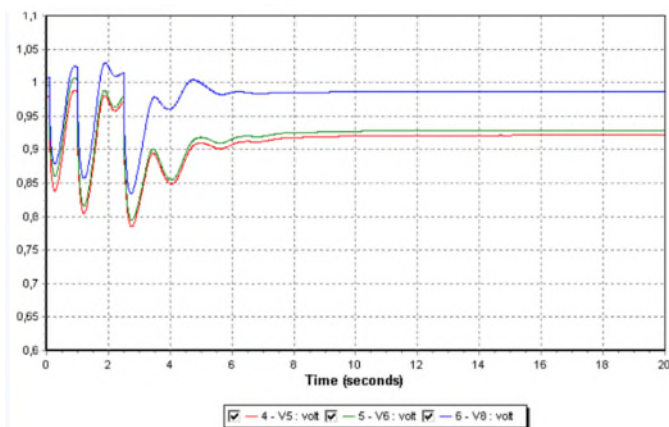


Figure. 10 Case 4: Load bus voltages before SVC installation.

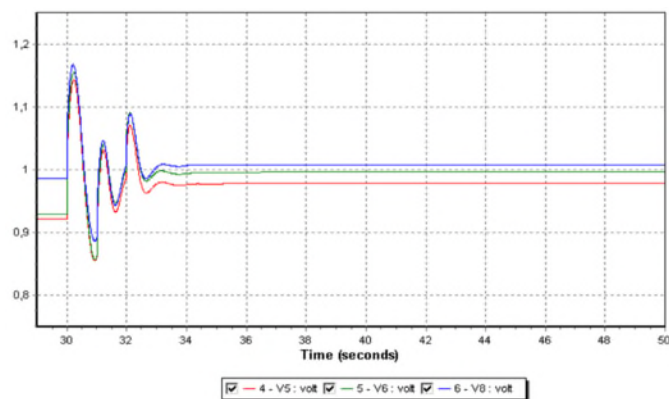


Figure. 11 Case 4: Load bus voltages after SVC installation.

6. CONCLUSIONS

The simulation results obtained for the four different disturbance sizes are highly satisfactory and align well

with previous research findings. It can be confidently stated that placing SVCs based on voltage sensitivities significantly enhances the voltage profile of the power system. Multiple cases have been examined in this study.

In the initial case study, the disturbance magnitude was exceedingly small. The voltage values remained within safe margins, and the system was able to rectify the disturbance using spinning reserve without necessitating SVC installation. In the second case study, the disturbance remained small, and this led to only minor impacts on the load bus voltages. However, in the third and fourth cases, the magnitude of the disturbance was substantial, resulting in voltages dropping to unacceptably low levels.

Nonetheless, upon implementing SVCs, an observable enhancement in the voltage profiles has been noted. Overall, it takes approximately 20 seconds for the system to attain an acceptable voltage level.

Determining the most optimal placement entails considering both voltage stability and real/reactive power losses. Consequently, the application of SVCs in power systems not only bolsters voltage stability but also curtails line losses and augments voltage regulation.

REFERENCES

- [1] Kothari, D. P. and Nagrath, I. J. (2006). Modern Power System Analysis, 3rd Edition, McGraw Hill, New York.
- [2] Kothari, D. P. and Nagrath, I. J. (2007). Power System Engineering," 2nd Edition, Tata McGraw Hill, New Delhi,
- [3] Santiago-Luna, M.; Cedeno-Maldonado, J.R, (2006). Optimal Placement of Facts Controllers in Power Systems via Evolution Strategies, Transmission & Distribution Conference and Exposition: Latin America, TDC '06. IEEE/PES, 15-18 August, pp. 1-6.
- [4] Pisica, I. Bulac, C. Toma, L. Eremia, M. (). Optimal SVC placement in electric power systems,
- [5] Hingorani, N.G. and Gyugyi, L. (2000). Understanding FACTS: Concepts and Technology of Flexible ac Transmission Systems, IEEE Press, Piscataway, NJ.
- [6] Song, Y.H. and Johns, A.T. (1999). Flexible ac transmission systems (FACTS) IEEE Power Engineering Society.
- [7] Hameed Al- Rubaiy, R. and Khalid Al- Jubor, W. (2016). Study and Simulation of IEEE 9 Bus System with UPFC for Transient Stability Analysis, JOURNAL OF APPLIED SCIENCES RESEARCH, 12(8): pages 36-48.



A new Algorithm for Image encryption based on chaotic systems

Djamel herbadji ^{1*}, Aïssa Belmeguenai¹, Derouiche Nadir¹, Abderahmane herbadji ²

¹Department of Electrical Engineering, 20 Aout 1955 University, Skikda 21000, Algeria

²Department of Electrical Engineering, msila University, msila 28000, Algeria

Corresponding Author Email: herbadjidjamel@gmail.com

ABSTRACT

In recent years, the use of chaotic maps in encryption has become an attractive research area, due to its numerous advantages, this make it very suitable for use in cryptography. In this paper we present a new image encryption algorithm based on confusion-diffusion process, Logistic-Logistic System is used to change the image pixel positions and values and Sin-Sin system is used to change the image pixel value. Satisfactory security performances are attained by only one encryption round, the algorithm have been validated using security analysis, and the experimental results demonstrate that the algorithm is simple, efficient and has properties of large key space, high sensitivity to its key.

Received: 20/02/2023

Accepted: 27/07/2023

Published: 19/09/2023

Keywords:

Image Encryption, chaotic map ,Logistic-Logistic, Sin-Sin, Sensitivity ;

1. INTRODUCTION

As mentioned in the abstract section, it will be rather easy to follow these rules as long as you just replace the “content” here without modifying the “form”.

As an important technology to protect the image content, image encryption has become an urgent challenge and high concern which has attracted many researchers in recent years. On the other hand chaotic systems have some good features, such as its extremely high sensitivity dependence on initial conditions and control parameters, nonlinearity, ergodicity and random-like behaviors[1],[2], on the other hand, the security of image encryption scheme that used the output sequences of chaotic maps usually depends on two parts, namely the permutation and the diffusion process [1-6]. In the permutation process, the pixel locations of the images are changed to remove the redundancies and break the high correlation among adjacent pixels, while in the diffusion process, the pixel values of the image are changed, some encryption schemes iterate these process to increase the effectiveness of encryption, many chaos-based image encryption algorithms have been recently proposed to prevent unauthorized access, such is the work of Zang et al.[3]they have proposed a multiple-image encryption algorithm based on mixed image element and permutation. Rim Zahmoul et al.[4], proposed an image encryption based on new Beta chaotic maps, where these maps have been used for generating chaotic sequences which are used in the

encryption scheme. Asia Mahdi et al.[5]proposed a Color Image Encryption and Decryption using Pixel Shuffling with the Henon Chaotic System, Yannick Abanda et al.[6]proposed an Image encryption by chaos mixing.

This work proposes a new algorithm to the encryption of image intended to be transferred on an insecure channel. The algorithm is simple and very easy to implement for image encryption and decryption. This paper is organized as follows; the first section is a historical introduction, the second section presents the chaotic maps. In the third section, the new proposed image algorithm will be presented in details. In the fourth section we present the experimental results and finally the conclusion is given in section 5.

2. CHAOTIC SYSTEMS

Logistic map and Sine map are the most famous 1D chaotic maps, which have simple and classic dynamical nonlinear equation with complex chaotic behaviors, they can be expressed by the following equations[7]:

$$X_{n+1} = rX_n(1 - X_n) \quad (1)$$

$$X_{n+1} = r\text{Sin}(\pi X_n) \quad (2)$$

Where ‘r’ is a control parameter with range of $r \in [0, 4]$ and X_n is the output chaotic sequence. From their bifurcation diagram presented in Figs.1(a) and Figs.1(b). We can see two defects in these chaotic maps, first, its chaotic range is limited. Second, as shown in Fig.1(a), Fig.1(b), their chaotic range is bounded only within [3.57, 4] and the control parameter ‘r’ is beyond this range, it cannot be considered as chaotic behaviors and non

uniform distribution of the output chaotic sequences that effected the distributions of encrypted image data and the performance of encryption system. A new chaotic maps have been proposed in[8] to solve the defects mentioned in above by combining these logistic maps as following.

2.1 Sine-Sine-Map

The Sine-Sine-System (SSS) is produced by combining the Sine map by using the following equation:

$$x_{n+1} = u \sin(\pi x_n)2^k - \text{floor}(u \sin(\pi x_n)2^k) \quad (3).$$

Where $\mu \in [0, 10]$ and $k \in [8, 20]$ are the control parameters of the new chaotic system map.

2.2 Logistic-Logistic-Map

The Logistic-Logistic-System(LLS) is produced by combining the logistic map by using the following equation:

$$x_{n+1} = u_n(1 - x_n)2^k - \text{floor}(u_n(1 - x_n)2^k) \quad (4)$$

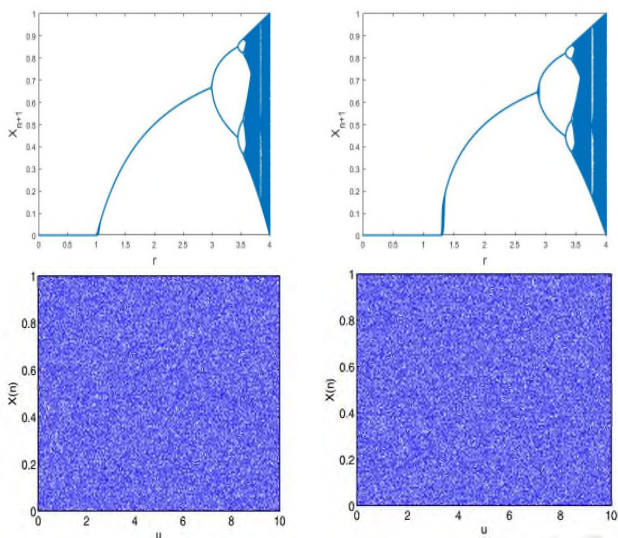


Fig.1. The bifurcation diagrams (a) Logistic map,(b) Sine map, (c) LLS, (d) SSS

The bifurcation diagram of LLS and SSS are illustrated in Fig.1(c) and Fig.1(d) respectively and [8]. Where their chaotic range is within $[0, 10]$, it is much larger than that of their seed maps, it has good chaotic performance.

3. PROPOSED IMAGE ENCRYPTION SCHEME

In this section, we propose a new image encryption algorithm. The encryption algorithm uses seven parameters of ($x_{0,1}=0.56, x_{0,2}=0.23, u_{0,1}=5.4321, u_{0,2}=2.81, k_1=14, k_2=14, p_1$) as the security key. The diagrams of the proposed encryption algorithm are shown in Fig.2 and 3.

3.1 Encryption process

Input: Plain image I with a size of $W \times H$.

Output: The ciphered image C with the same size.

Step 1: The grayscale image I is Reshaped into one vector $O = \{o_1, o_2, \dots, o_{W \times H}\}$ with the size of $W \times H$.

Step 2: Two different chaotic sequences are generated

$X_1 = \{x_{1,1}, x_{1,2}, \dots, x_{1,W \times H}\}, X_2 = \{x_{2,1}, x_{2,2}, \dots, x_{2,W \times H}\}$ of size $W \times H$, by using the equations 3 and 4 respectively. Then x_1 is arranged in ascending order then get the shuffled positions matrix x' , the process is shown in Fig.3.

Step 3: The image O is shuffled using x' to get the shuffled image P in order to break the correlation among

neighboring pixels and enhance the security of the scheme, by using the following equation

$$P(i) = O(x'(i)). \quad (5).$$

The diffusion process of the proposed scheme is detailed in Algorithm 1 and figure 3, which takes three inputs: a secret key K, the first pixel of the shuffled image $p_1 \in \{0, 256\}$, and the shuffled image P are produced as output a cipher-image $C = \{c_1, c_2, \dots, c_{W \times H}\}$. In our algorithm, every encrypted-pixel is related not just to the original pixel that generate it, but to all the other pixels. Therefore a small change in any original image pixel leads to a completely different encrypted image.

Algorithm 1 diffusion

```

1 input: Shuffled_image: P; secret_parameters:
    $x_{0,2}, u_{0,2}, k_2, p_1$ 
2 output: Cipher_image: C
3  $x_{0,2}, u_{0,2}, k_2$  are used to obtain a chaotic sequence
    $X_2$  of size  $H \times W$  using LLS
3  $X_2$  is converted to a sequence of integers values,
   by following equation
4  $X_2(i) = \text{floor}(X_2(i) * 10^{15}), 256)$ 
5  $n = H * W$ 
6  $Z(1) = p_1 \oplus X_2(1)$ 
7  $Z(n) = P(n) \oplus X_2(n)$ 
8  $P(n) = Z(n) \oplus Z(1)$ 
9 for  $i = 1 : n - 1$ 
10  $Z(i) = P(i) \oplus X_2(i)$ 
11  $C(i) = Z(i) \oplus Z(i + 1)$ 
12 end
13 The encrypted C is Reshaped into 2D matrix
   with size  $W * H$ 

```

The obtained image is a noise-like encrypted image.

3.1 Decryption process

The decryption process is the inverse of encryption process. The permutation and diffusion process used in decryption are as follows

$$O(x'(i)) = P(i);$$

Algorithm 2 invrse_diffusion

```

1 input: cipher_image C; secret_parameters:
    $x_{0,2}, u_{0,2}, k_2, p_1$ 
2 output: Shuffled_image: P
3  $x_{0,2}, u_{0,2}, k_2$  are Used to obtain a chaotic sequence
   X of size  $H \times W$  using LLS
4 X is converted to a sequence of integers values,
   by following equation
5  $X(i) = \text{floor}(X(i) * 10^{15}), 256)$ 
6  $n = H * W$ 
7  $Z(n) = C(n) \oplus X_2(n)$ 
8  $P(r * c) = [C(r * c) \oplus X_2(r * c)] \oplus [P(1) \oplus X_2(1)];$ 
9 for  $i = 1 : n - 1$ 
10  $P(i) = [C(i) \oplus X_2(i)] \oplus [P(i + 1) \oplus X_2(i + 1)];$ 
11 end

```

4. EXPERIMENTAL RESULTS

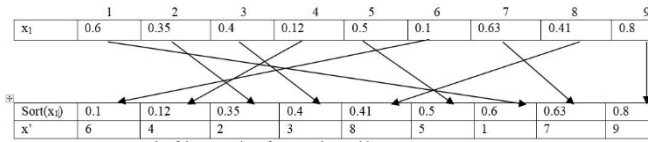


Fig.2. An example of permutation position vector generation

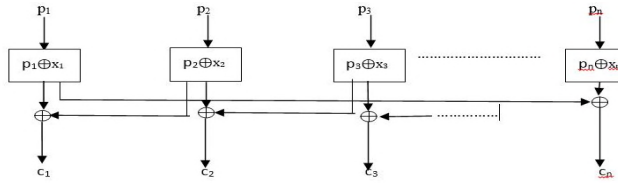


Fig.3. An example of the diffusion model of the proposed scheme

There are many kinds of attacks, such as statistical attacks and differential attacks [9]. In this section we will discuss the performance of the proposed algorithm through the obtained results; we will also use some types of tests to measure the performance of the proposed algorithm. The quantities to be measured are:

The number of pixel change rate (NPCR), the unified average changing intensity (UACI), the correlation analysis, and the PSNR (peak signal to noise ratio) and MSE (mean square error) tests, key space, key sensitivity and information entropy evaluation.

4.1 Key space analysis

In order to ensure that brute force attack infeasible, key space should be greater or less than 2^{100} [10]. The secret keys that is used in our proposed scheme are summarized as:

1- The control parameters $u_{0,1}, u_{0,2}$.

2- The initial values x_1, x_2 , the first pixel of shuffled image $p_1 \in [0, 255]$ and $k_1 \in [8, 20], k_2 \in [8, 20]$, if the space of each parameter and the initial value is set to 15 decimals, so the key space of our proposed scheme is $12 \cdot 12 \cdot 256 \cdot 10^{4 \cdot 15}$. It is large enough to resist to the brute force attack.

4.2 The histogram analysis

The image histogram illustrates the distribution of pixel values of its pixels[11]. To resist to statistic attacks, the image histogram should be fairly uniform. Fig. 4 and 5 display the histograms of the some plain-images and the histograms of their cipher-images. From Fig. 4 and 5, the histogram of the cipher-images is fairly uniform and flat distribution, so that it is enough to makes statistic attacks infeasible.

4.3 Information entropy analysis

Entropy is the most significant characteristic to measure the unpredictability and randomness measurements of information [12], the ideally entropy close to 8 for greyscale image [13]. Entropy of image I is defined as:

$$E(m) = - \sum_{i=0}^{255} \Pr(mi) \log_2 \Pr(mi). \quad (7).$$

Where $\Pr(mi)$ denotes the probability of symbol mi . The Information Entropy values of different encrypted image by using our scheme is listed in Table 1, and it refers that the entropy of the proposed encrypted images is all close to ideally entropy 8 and they are all greater than the

Information Entropy values obtained by [1][8]. The proposed encryption method is secure upon the entropy attack.

Table1: Information entropy analysis of various images

Image	Original	Encrypted	[1]	[8]
Lena	7.5691	7.9970	7.9972	7.9964
Boat	7.1913	7.9992	7.9992	7.9989
Barbara	7.6879	7.9992	7.9992	7.9989
Baboon	7.3579	7.9993	7.9992	7.9996

4.1 Coefficient correlation

In any image, each pixel have a high correlation with its adjacent pixels either in, vertical, diagonal or horizontal direction [12]. Therefore, an efficient image encryption algorithm should encrypt the images with sufficiently low correlation in the neighboring pixels. The correlation values

can be calculated by the following equation:

$$\text{corr} = \frac{\text{cov}(x,y)}{\sqrt{D(x)D(y)}}$$

Where X and Y are the sets composed of N pixel gray values, $x_i \in X$ and $y_i \in Y$, are two adjacent pixels,

$$E(X) = \frac{1}{N} \sum_{i=1}^N x_i, D(X) = \frac{1}{N} \sum_{i=1}^N [x_i - E(X)]^2 \quad \text{and}$$

$$\text{cov}(X, Y) = \frac{1}{N} \sum_{i=1}^N [x_i - E(X)][y_i - E(Y)].$$

The correlations among neighboring pixels at horizontal, vertical and diagonal directions of the plain image and its corresponding encrypted image have been displayed in Fig. 6. The correlation coefficients according to all directions of some images are listed in table 2. It can be seen that the encrypted image is very close to 0. Furthermore, we have compared our proposed algorithm to the one used in ref [1], ours has the smallest correlation values in all directions therefore, the proposed algorithm protects the images against statistical attacks.

Table 2. Coefficient Correlation Analysis.

Direction	Plain-Image	Cipher-Image	[1]
Diagonal	0.9346	-3.3846e-04	0.001949
Horizontal	0.9693	-0.0012	0.039886
Vertical	0.9179	-0.0012	0.034475

4.1 Key sensitivity analysis

In addition to the encryption algorithm has key space enough to resist to the brute force attack, also the encryption algorithm should be sensitive to their keys, where even there is only a slight difference of 10^{-14} between the encryption and decryption keys leads to failure of decryption. To evaluate the key sensitivity of our proposed algorithm, we decrypted Lena image with an incorrect independent parameter, the results are shown in Fig.7. We observe that for only a slight change of 10^{-14} , the decrypted image is absolutely different from the original image. This demonstrates that our proposed algorithm is very sensitive to their keys.

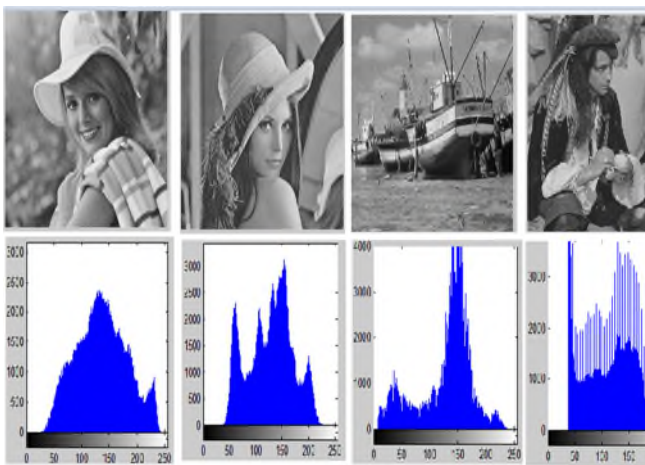


Fig. 4. Original images of 'Elaine', 'Lena', 'Boat', 'Man' and their histograms.



FIG. 7. Results of the key sensitivity. (a) Decrypted image with Correct key ; (b) decrypted image with $u_1 + 10^{-15}$; (c) decrypted image with wrong k_2 , (d) decrypted image with wrong p_1 ;

5. CONCLUSIONS

In this paper, a novel algorithm has been proposed for encryption images by using two chaotic maps. Logistic-logistic system has been used to change the positions of pixels of the image and the sine-sine System has been used to generate a sequence of random values that uses bit XOR operation for changed pixel value of image.

Differential and statistical analyzes have been conducted, the obtained results demonstrate the robustness of the algorithm against many of the known attacks.

REFERENCES

- [1] G. Ye, C. Pan, X. Huang, Z. Zhao, and J. He, "A Chaotic Image Encryption Algorithm Based on Information Entropy," *International Journal of Bifurcation and Chaos*, vol. 28, no. 1, p. 1850010, 2018.
- [2] R. Parvaz and M. Zarebnia, "A combination chaotic system and application in color image encryption," *Optics & Laser Technology*, vol. 101, pp. 30–41, 2018.
- [3] X. Zhang and X. Wang, "Multiple-image encryption algorithm based on mixed image element and permutation," *Optics and Lasers in Engineering*, vol. 92, pp. 6–16, 2017.
- [4] R. Zahmoul, R. Ejbali, and M. Zaied, "Image encryption based on new Beta chaotic maps," *Optics and Lasers in Engineering*, vol. 96, pp. 39–49, 2017.
- [5] A. M. N. Alzubaidi and N. D. K. Al-Shakarchy, "Color Image Encryption and Decryption Based Pixel Shuffling with 3D Blowfish Algorithm," *International Journal of Science and Research (IJSR)*, vol. 3, no. 7, pp. 336–343, 2014.
- [6] Y. Abanda and A. Tiedeu, "Image encryption by chaos mixing," *IET Image Processing*, vol. 10, no. 10, pp. 742–750, 2016.
- [7] Y. Zhou, L. Bao, and C. L. P. Chen, "A new 1D chaotic system for image encryption," *Signal processing*, vol. 97, pp. 172–182, 2014.
- [8] C. Pak and L. Huang, "A new color image encryption using combination of the 1D chaotic map," *Signal Processing*, vol. 138, pp. 129–137, 2017.
- [9] M. Dridi, M. A. Hajjaji, B. Bouallegue, and A. Mtibaa, "Cryptography of medical images based on a combination between chaotic and neural network," *IET Image Processing*, vol. 10, no. 11, pp. 830–839, 2016.
- [10] G. Alvarez and S. Li, "Some basic cryptographic requirements for chaos-based cryptosystems," *International Journal of Bifurcation and Chaos*, vol. 16, no. 8, pp. 2129–2151, 2006.
- [11] A. Beloucif, O. Noui, and L. Noui, "Design of a tweakable image encryption algorithm using chaos-based schema," *International Journal of Information and Computer Security*, vol. 8, no. 3, pp. 205–220, 2016.
- [12] W. Liu, K. Sun, Y. He, and M. Yu, "Color Image Encryption Using Three-Dimensional Sine ICMIC Modulation Map and DNA Sequence Operations," *International Journal of Bifurcation and Chaos*, vol. 27, no. 11, p. 1750171, 2017.
- [13] X. Chai, "An image encryption algorithm based on bit level Brownian motion and new chaotic systems," *Multimedia Tools and Applications*, vol. 76, no. 1, pp. 1159–1175, 2017.
- [14] M. Essaid, I. Akharraz, A. Saaidi, and A. Mouhib, "A New Image Encryption Scheme Based on Confusion-Diffusion Using an Enhanced Skew Tent Map," *Procedia Computer Science*, vol. 127, pp. 539–548, 2018.



Based Security Control of Networked Control System under Communication Constraints

Nafir Nourreddine ^{1*}, Rouamel Mohamed ², Bourahala.Faycal³

n.nafir@univ-skikda.dz,rouamel@univ-skikdadzf.bourahala@univ-skikda.dz

¹ Department of Electrical Engineering, LRES Laboratory, 20 Août 1955 University, Skikda, Algeria

^{2,3} Department of Electrical Engineering, LAS Laboratory, 20 Août 1955 University, Skikda, Algeria

Corresponding Author Email:n.nafir@univ-skikda.dz

ABSTRACT

Received: 20/02/2023

Accepted: 27/06/2023

Published: 19/09/2023

Keywords:

Security,Time-delay,stability,Linear matrix inequalities, Stabilization.

In this paper we deal with the security stability when a communication canal is inserted in the control loops which bring some communication constraints such as induced time delays and packets dropout. Those constraints can degrade the performances of the system or take it to instability that is to say that the control system is not secured. With the aim to keep good performances of the controlled system face of possible changes introduced by the network, it is interesting to introduce new approaches or ameliorate and improving some existing results. In this article we are concerned with the security function of the system with stability analysis and stabilization of networked control systems with network induced time-delay. To achieve this goal a novel augmented Lyapunov-Krasovskii functionals (LKF) is considered to derive the proposed delay dependent LMIs based secured stability conditions. Numerical examples and simulation results are presented to illustrate the effectiveness of the method.

1. INTRODUCTION

Feedback control systems wherein, actuators, sensors, controllers and other components are distributed around a digital communication network are called Networked Control Systems (NCSs), that can be shared or not with other applications [1][2][3]. Today's NCSs are widely used in many fields because of its appealing advantages, such as enabling remote data transmission, reducing the cabling complexity, minimizing costs and providing easy maintenance. Although NCSs have many attractive features, such as reduced wiring costs, ease of installation and maintenance and improved system reliability and efficiency, the insertion of a communication channel or network in the control loop has, on the other side, some challenging constraints which can degrade the performances of the control system and cause undesired stability problems[1][4][5].

The main issues addressed by the networked control system research community over the last twenty years are: Information loss and time delay [2-4]. Both constraints are causes for instability and performance degradation and the objective is to propose adequate methodologies for the modeling, analysis and design of networked systems that

are more complex than the traditional wired architecture [4][8].The issue packet dropouts arises in NCSs because analog signals are sampled, quantized and organized into information packets before transmission via the network according to specific data communication protocols.It is therefore necessary to propose appropriate control strategies for guarding a secured system function in presence of time delay and packet dropouts. The second issue is the network-induced delay, including sensor-to-controller delay and controller-to-actuator delay that occurs when data exchange happens among devices connected by the communication network, this delay, depending on the network characteristics such as network load, topologies, routing schemes, and it can be constant, time-varying, or even random [2,3].

The main objective of this thesis is to propose computationally efficient stability and stabilization criteria for linear networked control systems. We address systems with constant sampling rates, data packet losses, and varying time delays. In literature, most researches works dealt with time delay and packets dropout separately, in this context our first contribution is to take into account those two constraints simultaneously, by considering packet dropout as a time delay.

It is clear that the stability analysis and stabilization are important issues in analysis and design of networked control system with time delay. In general, there are two

ways for the stability analysis and control synthesis of time-delay NCSs models, they are delay-independent and delay-dependent approaches. For both approaches, they have their own advantages on dealing with time-delay NCSs models. Much attention has been paid to the study of delay-dependent stability and stabilization for time-delay systems because delay-dependent results for time-delay systems are less conservative than those for the delay-independent cases, especially for time-delay systems with actually small delay.

In this paper, we present a technique where the forward network-induced delay in the control loop is taken into consideration for the design of a stabilizing state feedback delay-dependent control law by resolution of a feasible set of linear matrix inequalities (LMIs)[8-10]. These LMIs are derived by using an appropriate Lyapunov functional for the closed-loop time-delayed system. The solution of the LMI control problem can be obtained using the LMI toolbox available in MATLAB.

The rest of the paper is organized as follows. The control problem is formulated in section II. Section III deals with the delay dependent conditions of state feedback stabilization. Numerical example and simulation are presented in section IV to illustrate the theoretical results, and conclusions are drawn in section V.

NOTATION.

In this paper, \mathbb{R}^n and $\mathbb{R}^{n \times m}$ denote, respectively, the n dimensional Euclidean space and the set of $n \times m$ real matrices. The superscript "T" denotes matrix transposition and the notation $X > 0$ (respectively, $X \geq 0$) where X is a symmetric matrix, means that X is positive definite (respectively, positive semi-definite). The symbol * will be used for symmetric terms in the LMIs.

2. PROBLEM STATEMENT

In this section, let us consider the following continuous-time system:

$$\begin{cases} \dot{x}(t) = Ax(t) + Bu(t) \\ y(t) = Cx(t) \end{cases} \quad (1)$$

Where:

$x(k) \in \mathbb{R}^n$, $u(k) \in \mathbb{R}^m$, $y(k) \in \mathbb{R}^l$ are states, control and output vectors of the system and $A \in \mathbb{R}^{n \times n}$, $B \in \mathbb{R}^{n \times m}$, $C \in \mathbb{R}^{m \times n}$ are known matrices. The system's initial condition is specified by $x(0) = x_0$.

The total variable time delay denoted by $\tau(t)$ is the sum of the two variable time delay from sensor to controller τ_1 and from controller to actuator τ_2 and will be assumed to satisfy:

$$\tau_{\min} \leq \tau(t) \leq \tau_{\max}$$

$$0 \leq \tau(t) \leq h, \quad \dot{\tau}(t) \leq \mu < \infty \quad (2)$$

With h and μ constant parameters.

In this paper, the goal is to investigate the control of the linear system (1), according to the networked control

scheme presented in Figure 1. In this context, we will consider the following assumptions.

ASSUMPTION1 All the state variables are available from measurements and transmitted to the controller

ASSUMPTION2 The sensors are clock driven; the controller and actuators are event driven

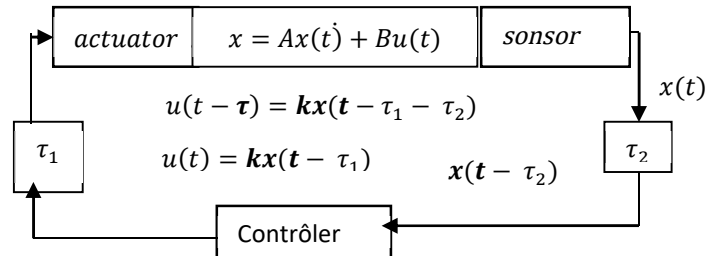


Figure1. Structure of the NCS with network-induced Time delay

To stabilize (1) over the network, let us consider the following sampled state feedback control law

$$u(t) = Kx(t) \quad (3)$$

Where k is the matrix gain and $\tau(t)$ is the total time delay to be computed with $\tau(t) = \tau_1 + \tau_2$. The objective is to design a state feedback controller given

$$u(t) = Kx(t - \tau(t)) \quad (4)$$

Such that the closed loop system shown in figure (1) is Asymptotically stable. Substituting the controller expression (3) into (1), we get the following closed-loop Dynamics:

$$\begin{cases} \dot{x}(t) = Ax(t) + BKx(t - \tau(t)) \\ x(s) = \varphi(s), \quad -h \leq s \leq 0 \end{cases} \quad (5)$$

3. MAIN RESULTS

In this section, we will first focus on the stability analysis of the closed-loop NCS (7) (assuming the controller gain K known). Then, the stability conditions will be convexified to allow the design of the controller gain K .

3.1 DELAY-DEPENDENT STABILITY CONDITION

This section presents new delay-dependent stability conditions of NCS time-delay models. The following lemmas are useful to obtain our results.

Lemma 1[1]: For any constant matrix $M > 0$, any scalars a and b with $a < b$, and any vector function $x(t) : [a, b] \rightarrow \mathbb{R}^n$ such that the integrals concerned are well defined, then, the following inequality holds:

$$\left[\int_a^b x(s) ds \right]^T M \left[\int_a^b x(s) ds \right] \leq (b - a) \int_a^b x^T(s) M x(s) ds$$

Lemma2 [2]:For any constant matrices $Q_{11}, Q_{22}, Q_{12} \in R^{n \times n}$, $Q_{11} \geq 0, Q_{22} \geq 0, \begin{bmatrix} Q_{11} & Q_{12} \\ * & Q_{22} \end{bmatrix} \geq 0$, scalar $\tau(t) \leq \tau_0$ and vector function $\dot{x}: [-\tau_0, 0] \rightarrow R^n$ such that the following integration is well defined, then

$$-\tau_0 \int_{t-\tau_0}^t \begin{bmatrix} x^T(s) & \dot{x}^T(s) \end{bmatrix} \begin{bmatrix} Q_{11} & Q_{12} \\ * & Q_{22} \end{bmatrix} \begin{bmatrix} x(t) \\ \dot{x}(t) \end{bmatrix} ds \leq \begin{bmatrix} x(t) \\ x(t-\tau) \\ \int_{t-\tau(t)}^t x(t) ds \end{bmatrix}^T \begin{bmatrix} -Q_{22} & Q_{22} & -Q_{12}^T \\ Q_{22} & -Q_{22} & Q_{12}^T \\ -Q_{12} & Q_{12} & -Q_{11} \end{bmatrix} \begin{bmatrix} x(t) \\ x(t-\tau) \\ \int_{t-\tau(t)}^t x(t) ds \end{bmatrix}$$

NEWTON-LEIBNITZ FORMULA

The Newton-Leibnitz Formula gives us

$$\int_{t-\tau(t)}^t \dot{x}(t) dt - x(t - \tau(t)) - x(t) = 0$$

For any appropriately dimensioned matrices N1 and N2, the following is true:

$$2[\dot{x}^T(t)N_1 + x^T(t - \tau(t))N_2] [x(t) - \int_{t-\tau(t)}^t \dot{x}(t) dt - x(t - \tau(t))] = 0$$

In the next theorem, the terms on the left side of this equation are added to the derivative of the Lyapunov-Krasovskii functional. The FWMs, N1 and N2, indicate the relationships among the terms of the Newton-Leibnitz formula; and optimal values for them can be obtained by solving LMIs. The proposed LMI-based stability conditions of the NCS assuming the controller gain K known are summarized by the following theorem.

THEOREM 1 for given scalar τ and h as well as the given matrices K , the closed-loop system (4) is asymptotically stable if there exist positive definite matrices $P = P^T > 0, Q > 0, R > 0$ and $S > 0$ and, matrices W_1, W_2, W_3 Such that the following LMI holds:

$$M = \begin{bmatrix} M_{11} & M_{12} & M_{13} & M_{14} \\ * & M_{22} & M_{23} & M_{24} \\ * & * & M_{33} & M_{34} \\ * & * & * & M_{44} \end{bmatrix} < 0$$

Where:

$$M_{11} = A^T P + P^T A + Q + R - W_1 - W_1^T + h A^T S A$$

$$M_{12} = W_1^T - W_2 + P B K + h A^T S B K, M_{13} = -W_3,$$

$$M_{14} = W_1^T$$

$$M_{22} = -(1 - \mu) Q + W_2 + W_2^T + h K^T B^T S B K,$$

$$M_{23} = W_3, M_{24} = W_2^T,$$

$$M_{33} = -R, M_{34} = W_3^T, M_{44} = -\frac{1}{h} \cdot S$$

PROOF:To prove the theorem, let us propose the following Lyapunov-Krasovskii functional candidate:

$$V(x(t)) = V_1(x(t)) + V_2(x(t)) + V_3(x(t)) + V_4(x(t)) \quad (7)$$

Where

$$V_1(x(t)) = x^T(t) P x(t) \quad (8)$$

$$V_2(x(t)) = \int_{t-\tau(t)}^t x^T(s) Q x(s) ds \quad (9)$$

$$V_3(x(t)) = \int_{t-h}^t x^T(s) R x(s) ds \quad (10)$$

$$V_4(x(t)) = \int_{-h}^0 \int_{t+\theta}^t x^T(s) S \dot{x}(s) ds d\theta \quad (11)$$

REMARK

There are four important points regarding the Development of model transformations. When double-integral terms are introduced into the Lyapunov-Krasovskii functional to produce a delay-dependent stability condition, it results in quadratic integral terms appearing in the derivative of that functional. Model transformations emerged as a way of dealing with those quadratic integral terms. More specifically, the purpose of a model transformation is to bring the integral terms into the system equation so as to produce cross terms and quadratic integral terms in the derivative of the Lyapunov-Krasovskii functional. Then, the bounding of the cross terms eliminates the quadratic integral term.

The LKF candidate (7) is positive if P, Q, R, S, are all positive definite matrices. Moreover, the NCS model with network-induced delay is asymptotically stable if:

$$\dot{V}(x(t)) = \dot{V}_1(x(t)) + \dot{V}_2(x(t)) + \dot{V}_3(x(t)) + \dot{V}_4(x(t)) < 0$$

Calculating the derivative of $V(x(t))$ along the solution of system (3) yields

$$\dot{V}(x(t)) = \dot{V}_1(x(t)) + \dot{V}_2(x(t)) + \dot{V}_3(x(t)) + \dot{V}_4(x(t))$$

Where

$$\dot{V}_1(x(t)) = x^T(t) [A^T P + A P] x(t) + 2x^T(t) P B K x(t - \tau(t)) < 0 \quad (12)$$

$$\begin{aligned} \dot{V}_2(x(t)) &= x^T(t) Q x(t) \\ &- (1 - \dot{\tau}(t)) x^T(t - \tau(t)) Q x(t - \tau(t)) \\ &\leq x^T(t) Q x(t) \\ &- (1 - \mu) x^T(t - \tau(t)) Q x(t - \tau(t)) < 0 \end{aligned} \quad (13)$$

$$\dot{V}_3(x(t)) = x^T(t) R x(t) - x^T(t - h) R x(t - h) < 0 \quad (14)$$

$$\begin{aligned} \dot{V}_4(x(t)) &= h \dot{x}^T(t) S \dot{x}(t) - \int_{t-h}^t \dot{x}(s) S \dot{x}(s) ds \\ &\leq x^T(t) h A^T S A x(t) + x^T(t) h A^T S B K x(t - \tau(t)) \\ &+ x^T(t - \tau(t)) h K^T B^T S A x(t) \end{aligned}$$

$$+x^T(t - \tau(t))hK^T B^T S B K x(t - \tau(t)) - \frac{1}{h} \left(\int_{t-\tau(t)}^t \dot{x}(s) ds \right)^T S \left(\int_{t-\tau(t)}^t \dot{x}(s) ds \right) \quad (15)$$

So the final time derivative of Lyapunov Krasovskii function is given By

$$\begin{aligned} \dot{V}(x(t)) \leq & x^T(t)M_{11}x(t) + x^T(t)M_{12}x(t - \tau(t)) \\ & + x^T(t)M_{13}x(t - h) + x^T(t)M_{14} \left(\int_{t-\tau(t)}^t \dot{x}(s) ds \right) \\ & + x^T(t - \tau(t))M_{12}^T x(t) + x^T(t - \tau(t))M_{22}x(t - \tau(t)) \\ & + x^T(t - \tau(t))M_{23}x(t - h) \\ & + x^T(t - \tau(t))M_{24} \left(\int_{t-\tau(t)}^t \dot{x}(s) ds \right) \\ & + x^T(t - h)M_{13}^T x(t) + x^T(t - h)M_{23}^T x(t - \tau(t)) \\ & + x^T(t - h)M_{33}x(t - h) + x^T(t - h)M_{34} \left(\int_{t-\tau(t)}^t \dot{x}(s) ds \right) \\ & + \left(\int_{t-\tau(t)}^t \dot{x}(s) ds \right)^T M_{14}^T x(t) \\ & + \left(\int_{t-\tau(t)}^t \dot{x}(s) ds \right)^T M_{24}^T x(t - \tau(t)) \\ & + \left(\int_{t-\tau(t)}^t \dot{x}(s) ds \right)^T M_{34}^T x(t - h) \\ & + \left(\int_{t-\tau(t)}^t \dot{x}(s) ds \right)^T M_{44}^T \left(\int_{t-\tau(t)}^t \dot{x}(s) ds \right) \quad (16) \end{aligned}$$

As we can see the whole derivative contain some noun quadratic integral terms, those terms must be treated securely to get at least a quadratic from of the time derivative of the Lyapunov function.

By using lemma 1 and lemma2 and by exploiting Newton Leptniz formula,the expression ofthe time derivative of the Lyapunov function can be rewritten as follows:

$$\dot{V}(x(t)) \leq \eta^T(t)M\eta(t) \quad (17)$$

With

$$\eta(t) = [x^T(t) \ x^T(t - \tau(t)) \ x^T(t - h) \ \left(\int_{t-\tau(t)}^t \dot{x}(s) ds \right)^T]^T$$

Which indicates that the derivative $\dot{V}(x(t))$ is strictly negative and, the Lyapunov functional is decreasing ifficiency matrix M is negative definite. This completethe proof of theorem 3.1.

3.2. CONTROLLER DESIGN

The following theorem gives equivalent LMI condition for the design of the state feedback controller.

THEOREM 2

Let ϵ be a given positive scalar. There exists a stabilizing state feedback controller for the closed-loop networked

control system if there exist matrix $X > 0$, matrices $\bar{W}_1, \bar{W}_2, \bar{W}_3$ and matrices $\bar{Q} > 0, \bar{R} > 0$ and $\bar{S} > 0$ such that the following set of LMIs hold:

$$\bar{M} = \begin{bmatrix} \bar{M}_{11} & \bar{M}_{12} & \bar{M}_{13} & \bar{M}_{14} & XA^T \\ * & \bar{M}_{22} & \bar{M}_{23} & \bar{M}_{24}(BY)^T & \\ * & * & \bar{M}_{33} & \bar{M}_{34} & 0 \\ * & * & * & \bar{M}_{44} & 0 \\ * & * & * & * & -\frac{1}{\epsilon}X \end{bmatrix} < 0$$

$$h\bar{S} < \epsilon X, \epsilon > 0$$

Where

$$\begin{aligned} \bar{M}_{11} &= XA^T + AX + \bar{Q} + \bar{R} - \bar{W}_1 - \bar{W}_1^T, \\ \bar{M}_{12} &= \bar{W}_1^T - \bar{W}_2 + BY \\ \bar{M}_{13} &= -\bar{W}_3, \quad \bar{M}_{14} = \bar{W}_1^T, \\ \bar{M}_{22} &= -(1 - \mu)\bar{Q} + \bar{W}_2 + \bar{W}_2^T, \quad \bar{M}_{23} = \bar{W}_3, \quad \bar{M}_{24} = \bar{W}_2^T \\ \bar{M}_{33} &= -R, \quad \bar{M}_{34} = \bar{W}_3^T, \quad \bar{M}_{44} = -\frac{1}{h}\bar{S} \end{aligned}$$

The stabilizing controller gain is given by $K = YX^{-1}$. The proof of theorem2.Relies on finding equivalent LMI conditions based on the Schur complement theorem. For this purpose, note that the previous LMI can be rewritten:

$$M = \begin{bmatrix} \tilde{M}_{11} & \tilde{M}_{12} & \tilde{M}_{13} & \tilde{M}_{14} \\ * & \tilde{M}_{22} & \tilde{M}_{23} & \tilde{M}_{24} \\ * & * & \tilde{M}_{33} & \tilde{M}_{34} \\ * & * & * & \tilde{M}_{44} \end{bmatrix} + \begin{bmatrix} A^T \\ (BK)^T \\ 0 \\ 0 \end{bmatrix} [hs][A \ BK \ 0 \ 0] < 0$$

Where:

$$\begin{aligned} \tilde{M}_{11} &= A^T P + P^T A + Q + R - W_1 - W_1^T, \quad \tilde{M}_{34} = W_3^T \\ \tilde{M}_{12} &= W_1^T - W_2 + P B K, \quad \tilde{M}_{13} = -W_3, \quad \tilde{M}_{14} = W_1^T \\ \tilde{M}_{22} &= -(1 - \mu)Q + W_2 + W_2^T, \quad \tilde{M}_{24} = W_2^T \\ \tilde{M}_{33} &= -R, \quad \tilde{M}_{44} = -\frac{1}{h}S \end{aligned}$$

Letting $X = P^{-1}$ and, pre- and post-multiplying (12) by X we get: $h\bar{S} < \epsilon X, \epsilon > 0$ Where $\bar{S} < X.S.X$. Then, by Schur complement, (11) is equivalent to the following LMI:

$$\begin{bmatrix} \tilde{M}_{11} & \tilde{M}_{12} & \tilde{M}_{13} & \tilde{M}_{14} & A^T \\ * & \tilde{M}_{22} & \tilde{M}_{23} & \tilde{M}_{24}(BK)^T & \\ * & * & \tilde{M}_{33} & \tilde{M}_{34} & 0 \\ * & * & * & \tilde{M}_{44} & 0 \\ A & BK & 0 & 0 & -1/\epsilon P^{-1} \end{bmatrix} < 0 \quad (18)$$

Now, let $Y = KX$, $\bar{Q} = XQX$, $\bar{R} = XRX$, $\bar{W}_1 = XW_1X$, $\bar{W}_2 = XW_2X$ and $\bar{W}_3 = XW_3X$. Pre-and post-multiplying (18) by $\text{Diag}(X, X, X, X, I)$ yields the LMI condition. The set of LMIs (9) and (10) are linear in the unknown matrices $X, Y, \bar{W}_1, \bar{W}_2, \bar{W}_3, \bar{Q}, \bar{R}$ and \bar{S} can be solved using the LMI MATLAB toolbox and the stabilizing gain matrix is computed as $K = YX^{-1}$.

3. SIMULATION EXAMPLE

In This section, we present a numerical example to demonstrate the effectiveness and applicability of the proposed theory over an inverted pendulum system. The plant to study is sketched in Figure (2). The pendulum carried by a cart is allowed to rotate about its axis. The cart moves horizontally by means of a belt and a motor which applies a force $F(t)$. The mathematical model of the mechanical system is deduced by application of the fundamental principle of dynamics and the balance of forces involved. The cart position and the angle of the inverted pendulum are denoted by x and θ , respectively. The linearization of the system model about its equilibrium leads to the following linear time-invariant state space model where, the state vector is given by:

- x : cart position
- θ : Pendulum angle
- F : Force applied to the cart

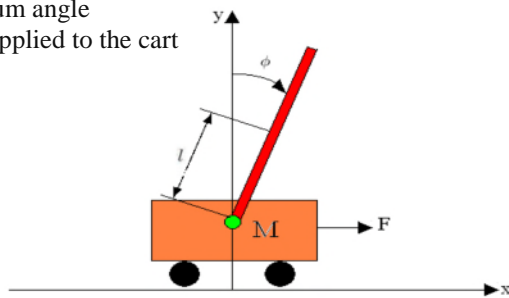


Figure (2): Structure of the linear inverted pendulum

$$[x_1 \ x_2 \ x_3 \ x_4]^T = [\theta \ \dot{\theta} \ x \ \dot{x}]^T$$

The physical linear model in the state space is given by :

$$\begin{bmatrix} \dot{x}_1 \\ \dot{x}_2 \\ \dot{x}_3 \\ \dot{x}_4 \end{bmatrix} = \begin{bmatrix} 0 & 1 & 0 & 0 \\ M + m/MI & 0 & 0 & 0 \\ 0 & 0 & 0 & 1 \\ -Mg/m & 0 & 0 & 0 \end{bmatrix} \begin{bmatrix} x_1 \\ x_2 \\ x_3 \\ x_4 \end{bmatrix} + \begin{bmatrix} 0 \\ -1/MI \\ 0 \\ 1/M \end{bmatrix} u$$

For simulation we will assume that $g = 9.81$; $m = 0.1kg$; $M = 2kg$; $2l = 1m$ in this case we get

$$A = \begin{bmatrix} 0 & 1 & 0 & 0 \\ 20.601 & 0 & 0 & 0 \\ 0 & 0 & 0 & 1 \\ -0.4905 & 0 & 0 & 0 \end{bmatrix}, B = \begin{bmatrix} 0 \\ -1 \\ 0 \\ 0.5 \end{bmatrix}$$

This system is open-loop unstable, where the state variables of the free system increase indefinitely from the initial state. However, this control law is unable to stabilize

the system when the sensor transmits the state information to the controller via a communication network that induces a delay of a maximum value $h = 60ms$ in the control loop, as shown in figure (3).

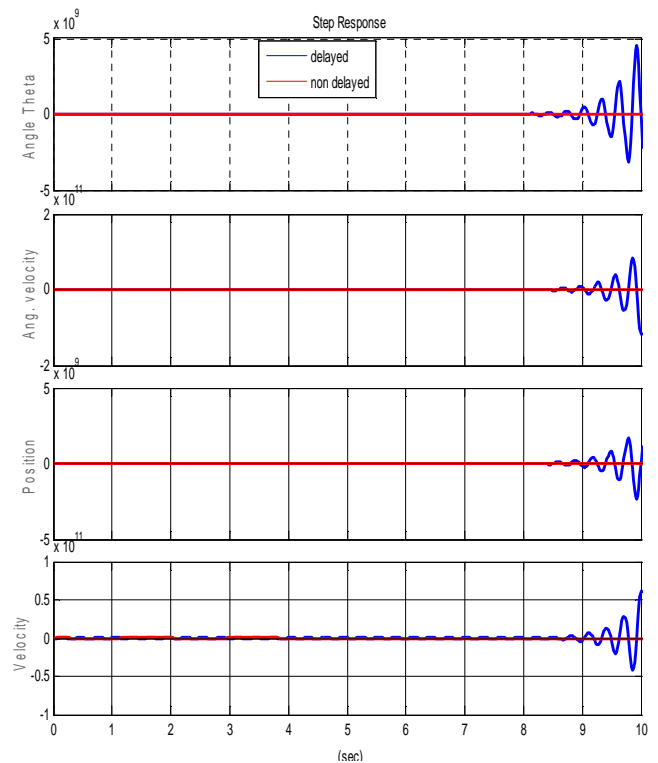


Fig. 3 Unstable closed-loop delayed system ($h=60ms$)

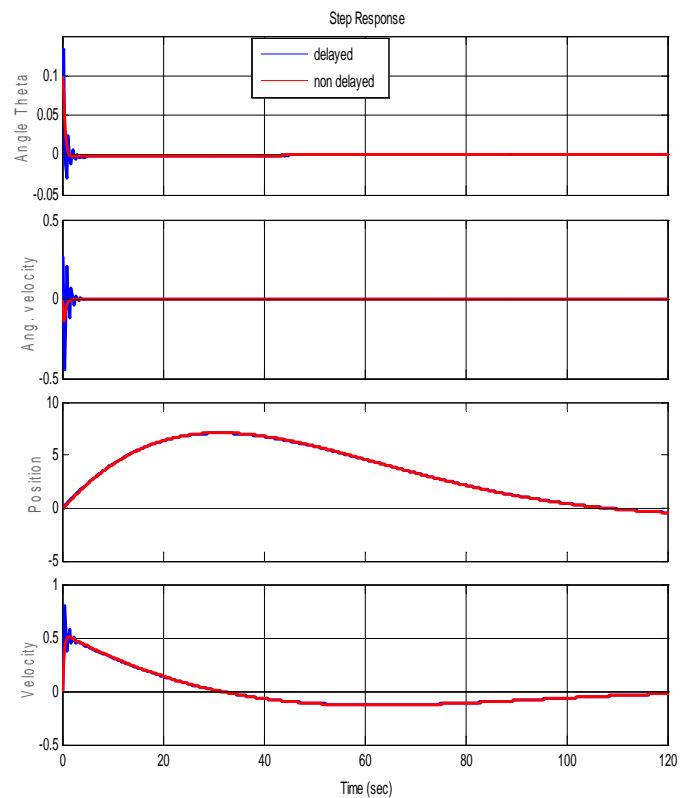


Fig. 4 Stable closed-loop system under network Induced Delay constraint ($h=125ms$)

The response of the closed-loop system with the designed control law and under initial conditions is shown in Fig.6 We can see the stable response of the system from the initial position, when driven by a controller gain matrix computed by applying the LMI technique developed in the theory. The stabilizing gain matrix is given by

$$K_{LMI} = [35.1561 \ 7.7472 \ 0.0020 \ 0.0671]$$

This controller is able to stabilize the inverted pendulum controlled via a communication network that induces a transmission delay varying in the interval 0ms to 125ms

4. Conclusion

This paper dealt with the secured stability and stabilization of networked control systems by state-feedback control under the constraint communication packet loss and delay induced in the sensor-to-controller path. The delay considered is time varying and bounded. The stabilization control problem is studied and sufficient conditions are derived in the form of linear matrix inequalities (LMIs). The sufficient conditions are delay-dependent. Future work includes extension to the general case of network-induced delays in both forward and backward paths.

5. REFERENCES

- [1] M. Rouamel, F. Bourahala, A. N.D. Lopes, N. Nafir, and K. Guelton.(2021) Mixed actual and memory data-based event-triggered H^∞ control design for networked control system. In 4th IFAC Conference on Embedded Systems, Computational Intelligence and Telematics in Control. Proceedings. CESCIT'21, pages 1–6.
- [2] L. Zhang, Y. Shi, T. Chen.(2005)A new method for stabilization of networked control systems with random delays. IEEE Transactions on Automatic Control, 50(8): 1177 – 1181.
- [3] Z. Zuo and Y. Wang. (2006). New stability criterion for a class of linear systems with time-varying delay and nonlinear perturbations. IEE Proceedings – Control Theory & Applications, 153(5): 623-626.
- [4] Fei-yue Wang, De Song Liu. (2008). Networked Control Systems theories and applications, Springer-Verlag London limited
- [5] Boyd, S., Ghaoui,L.,Feron,E.,Balakrishnan,V.(1994). Linear Matrix Inequalities in System and Control Theory. SIAM, Philadelphia.
- [6] Chonh lin, Quing-Guo Wang, tong Heng Lee ,Yong Hee (2007)LMI Approach to Analysis and Control of Takagi-Sugeno Fuzzy Systems With Time Delay, Springer-Verlag Berlin Heidelberg .
- [7] Min Wu ,Yong He,Jin-Hua She.(2010).Stability Analysis and Robust Control of Time-Delay Systems ,Springer-Verlag Berlin Heidelberg.
- [8] Chen Peng, Dong Yue, and Yu-Chu Tian.(2009).New Approach on Robust Delay-Dependent H^∞ Control for Uncertain T – S Fuzzy Systems With Interval Time-varying delay. IEEE transactions on fuzzy systems, vol. 17, no. 4, august 2009.
- [9] P. Chen, Y.C. Tian. Delay-dependent robust stability criteria for uncertain systems with interval time-varying delay. Journal of Computational and Applied Mathematics (2007)doi:10.1016/j.cam.2007.03.009.
- [10]K. Gu, V.L. Kharitonov, J. Chen.(2003) Stability of Time-Delay Systems, Birkhauser, Basel.
- [11] L. Xie,(1996).Output feedback control of systems with parameter uncertainty, International Journal of Control 63 (4) (1996) 741–750.
- [12] F. Bourahala, K.Guelton, and A. ND Lopes.(2019) Relaxed non-quadratic stability conditions for takagi-sugeno systems with time-varying delays: A wirtinger’s inequalities approach. In 2019 IEEE International Conference on Fuzzy Systems (FUZZ-IEEE), pages 1–6. IEEE.
- [13] F. Bourahala, M. Rouamel, and K. Guelton.(2021) Improved robust stability analysis and stabilization of uncertain systems with stochastic input time-varying Delays.Optimal Control Applications and Methods.
- [14] N. Nafir, Z. Ahmida, K. Guelton, F. Bourahala, and M. Rouamel. (2021)Improved robust h-infinity stability analysis and stabilization of uncertain and disturbed networked control systems with network induced delay and packet dropout.International journal of systems science.



Studies and Analysis of the MPPT based DISMC of PV using Buck Converter connected to Battery

Yousra Izgheche¹, Tahar Bahi²

¹Department of Electronic, Laboratory of Automatic and Signal Annaba , University Badji Mokhtar Annaba,

²Department of Electrotechnic, Laboratory of Automatic and Signal Annaba , University Badji Mokhtar Annaba,
izghecheyousra95@gmail.com & tbahi@hotmail.com

ABSTRACT

Received: 28/02/2023
Accepted: 28/07/2023
Published: 19/09/2023

Keywords:

Photovoltaic (PV), Buck converter, MPPT, P&O algorithm, DISMC , Battery, MATLAB, Simulink.

This paper presents a detailed modeling of the MPPT based on the DISMC technique applied to a stand-alone PV system with a DC-DC buck converter , to reveal the best performances experiencing fast convergence, fast transient response and robustness to variable climatic conditions, such as irradiation . Improving PV power requires robust MPP tracking. Most techniques used to achieve MPPT have some drawbacks , DISMC's strategy is to design a sliding surface that fixes the operating point. Reaching this surface in finite time requires a control law applied to the grid of the DC/DC converter. A buck converter is used as the DC-DC converter for the load system. It is used to match the impedance of the solar panel and the battery to provide maximum power. The objective of this work is to improvement of the power quality under different conditions . The simulation results on Matlab/Simulink are presented and discussed.

1. INTRODUCTION

The growing demand for electrical energy and the constraints associated with its production, such as pollution and the effects of global warming, have prompted research into the development of renewable energies. Among renewable energy sources, photovoltaic (PV) systems offer a highly competitive solution.

Interest in renewable energies continues to grow. Efforts are being made to develop clean, efficient and inexpensive energy sources. Solar energy has long been a key area of research, and research in this field continues to accelerate. Lead-acid batteries are still popular, although lithium-ion batteries are also being tested, but cost is the decisive factor. Solar energy is harnessed by stand-alone photovoltaic systems [1]. Photovoltaic panels convert solar energy into electricity. Photovoltaic systems have non-linear internal characteristics [2]. Irradiance, temperature and power characteristics in solar photovoltaic systems. Due to the high cost of photovoltaic panels, maximum power point tracking (MPPT) is required to track maximum power output [4]. DC/DC converters are connected to photovoltaic panels and batteries. Lead-acid batteries are the most commonly used because of their wide operating temperature range, low self-discharge, long service life and low maintenance requirements [5] . Batteries are cheaper to install than photovoltaic panels.

But compared with photovoltaic panels, the lifetime cost of batteries is higher [6].

Photovoltaic systems also have a limited service life. If the availability of photovoltaic energy is low for a long period, or if charging and discharging are inadequate, battery life will be shortened [7]. Or incorrect charging and discharging. Charging the battery The battery charge must be controlled to achieve a high state of charge and longer battery life [8]. (SOC) and longer battery life. The main objective is to charge the battery safely using solar energy. This report presents the modeling of an MPPT battery charge controller in Simulink [9]. A step-down converter supplying 12V to the battery. Power conversion Power conversion is performed by a step-down converter [10]. In the proposed system, a photovoltaic model, a battery model and a battery charging system designed with a step-down converter are implemented. It requires a DISMC control method to extract the maximum power point from MPPT.

The main aim of this study is to determine how the controller reacts to sudden variations in solar irradiance and temperature, to attenuate undesirable oscillations caused by DC/DC converter switching and/or the controller itself, and to determine the response time. The simulations were carried out using MATLAB-SIMULINK, and the results are presented in this report. The simulation is carried out using MATLAB/Simulink.

2. MODELING OF THE GPV

Figure 1 shows the method adopted in this report for charging batteries by detecting the battery charging current. MPP tracking systems are used to increase the maximum power produced by the solar panel. Even if temperature, irradiation and load characteristics vary, this keeps the output of the photovoltaic solar panel at a constant level. constant. For greater efficiency of the PV panel output, a buck converter is used to transmit DC-DC energy. In stand-alone photovoltaic systems, buck converters are effective in DC step-down and transmission operations and , battery storage . tracking solar energy from photovoltaic panels. PV panel, many MPPT techniques are available, disturbance and observation, incremental conductance algorithm, etc.. Among all the control algorithms, the DISMC method is the most efficient than simple control algorithms.

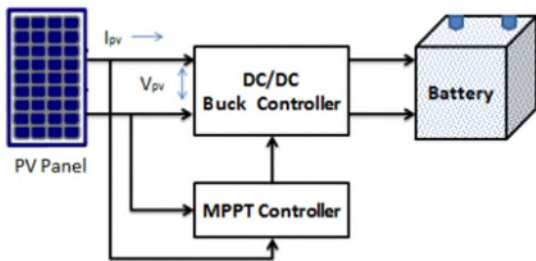


Figure. 1. Block diagram of the system

3. CHARACTERISTICS OF PV PANEL

The modeling of PV parameters is taken from the article [11-12]. The single-diode model is considered (See Figure 2) because of its advantages: simplicity of design and ease of analysis of PV performance. There are four parameters required to model the single diode circuit PV [13].

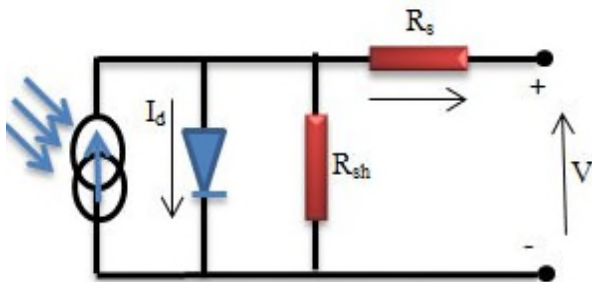


Figure.2 Equivalent diagram of a PV cell

$$I_{pv} = I_{ph} - I_0 \left[e^{\frac{q(V_{pv} + I_{pv}R_s)}{nkT}} - 1 \right] - \frac{V_{pv} + I_{pv}R_s}{R_{sh}} \quad (1)$$

Where,

I_{ph} :photocurrent;

I_0 :diodesaturationcurrent;

I_{pv} :terminalcurrent;

V_{pv} :voltageacrosstheoutputterminal; (5)

R_s :moduleseriesresistance;

R_{sh} :moduleshuntresistance;

N_s : number of cells in one module ;

n: diodeidealityfactor ;

k : Boltzmann’s constant ;

T : absolutetemperature;

q:elementarycharge;

Le logiciel MatLab/Simulink est utilisé pour la programmation des cellules PV et des GPV. Les caractéristiques I-V et P-V. sont illustrées par la figure 3.

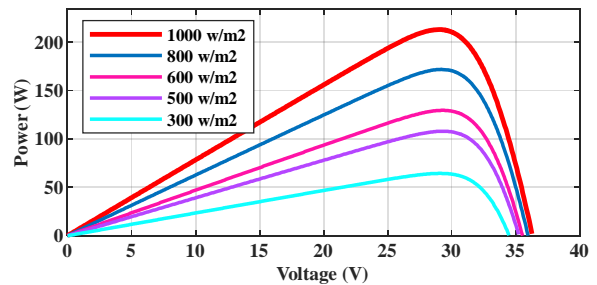
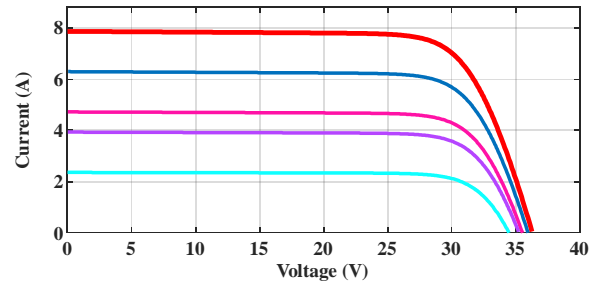


Figure . 3.Variation in P-V curves

4. MPPT BASED DOUBLE INTEGRAL SLIDING MODE CONTROLLER

For maximum power output, the proposed MPPT model based on DISMC is implemented in Matlab/Simulink. This algorithm was developed to eliminate the chatter caused by inverter switching, which is expressed as a nuisance, when unwanted disturbances occur in PV systems[14] . The sliding mode control system consists of two main parts, the first part consists of extracting the sliding surface through the parameters provided by the DC-DC converter, the second part is the formulation of the control law to drive and maintain the system towards the sliding surface[15] .

The sliding mode $S(t)$ is defined by :

$$S(t) = \{x \setminus S(x, t) = \dot{S}(x, t) = 0\} \quad (2)$$

The sliding surface is chosen to provide maximum output power. The sliding surface is defined by :

$$\left(\frac{\partial P_{pv}}{\partial I_{pv}} \right) = 0, \quad \left(\frac{\partial P_{pv}}{\partial I_{pv}} \right) = I_{pv} \left(\left(\frac{\partial V_{pv}}{\partial I_{pv}} \right) + \left(V_{pv} / I_{pv} \right) \right) \quad (3)$$

La surface de glissement est la suivante :

$$S(t, x) = \left(\left(\frac{\partial V_{pv}}{\partial I_{pv}} \right) + \left(V_{pv} / I_{pv} \right) \right) \quad (4)$$

For the controller design, the tracking error e is given as follows in equations (5) and (6) :

$$S(x) = e(x), \quad e(x) = e(x_1) + e(x_2)$$

$$e(x_1) = \int (\Delta P / \Delta t) dt, \quad e(x_2) = \int \left\{ \int (\Delta P / \Delta t) dt \right\} dt, \quad \begin{cases} \Delta P = P_{pv}(k) - P_{pv}(k-1) \\ \Delta I = I_{pv}(k) - I_{pv}(k-1) \end{cases} \quad (6)$$

Typically, the sliding-mode control law is composed of two terms, the equivalent control term and the discontinuous control term. The DISMC algorithm is used to stabilize the system and push it towards convergence to the desired path at the right time[16].

$$u = u_{eq} + u_n \tag{7}$$

In order to obtain equivalent control, the stability condition must be ensured

$$\begin{cases} S(x) = 0 \\ \dot{S}(x) = 0 \end{cases} \Rightarrow u \cong u_{eq} \tag{8}$$

The equivalent control can be obtained by solving the following algebraic equation:

$$\dot{S} = [dS / dx]^T, \quad \dot{x} = [dS / dx]^T \cdot (f(x) + g(x)u_{eq}) \tag{8}$$

$$u_{eq} = -([dS / dx]^T f(x)) / ([dS / dx]^T g(x)) = 1 - (K_1 [S + V_{pv}] / V_s) \tag{9}$$

Taking into account that discontinuous control to ensure the Lyapunov stability criterion is possible [17], this is given by :

The expression of the discontinuous control law is given by :

$$u_n = K_2 \cdot |S|^\alpha \cdot \sin g(S), \quad 0 < \alpha < 1 \tag{10}$$

$$\begin{cases} \sin g(S) = 1 & \text{if } S(x) > 0 \\ \sin g(S) = 0 & \text{if } S(x) = 0 \\ \sin g(S) = -1 & \text{if } S(x) < 0 \end{cases} \tag{11}$$

$$u = u_{eq} + u_n = [1 + K_2 \cdot |S(x)|^\alpha \cdot \sin g(S) - (K_1 [S(x)dx + V_{pv}] / V_s)] \tag{12}$$

Where K₁ and K₂ are positive constants

5.DC-DC BUCK CONVERTER

The DC-DC converter converts the DC input voltage source into a higher or lower output voltage. Since the PV generator voltage is higher than the battery voltage, the basic topology of a dc-dc buck converter is illustrated in figure 5. , and consists of a controlled SW switch, an uncontrolled switching diode (D), an inductance L, a capacitance C and a load resistor R .Table 1 shows the parameters used .

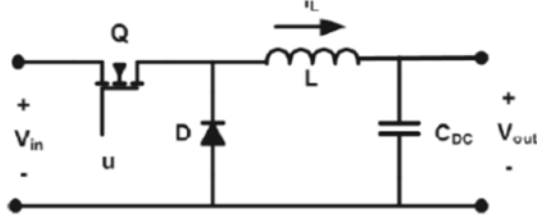


Figure. 4 Buck Converter.

Table 1. Buck converter specification:

Parameter	Value
C ₁	1 mF
C ₂	369.79 μF
L	0.8653 mH

5. DISCUSSIONS AND RESULTS

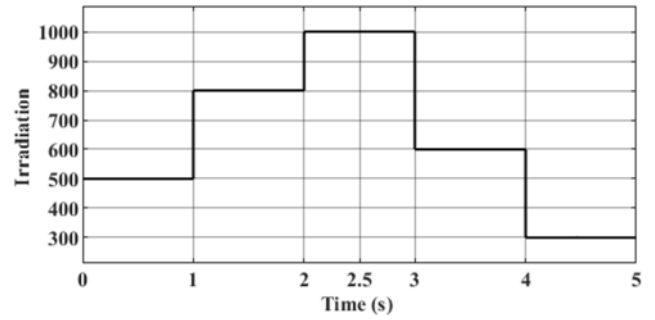


Figure. 5 profil of Irradiation

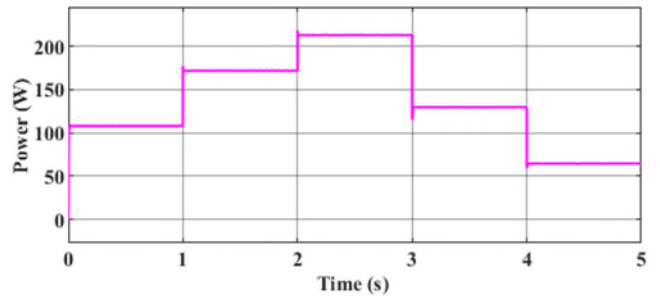


Figure. 6 Power of the PV

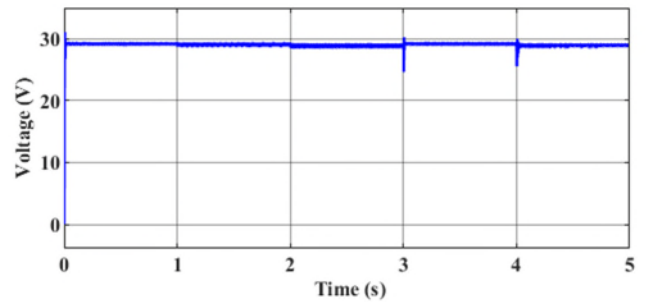


Figure. 7 Voltage of the PV

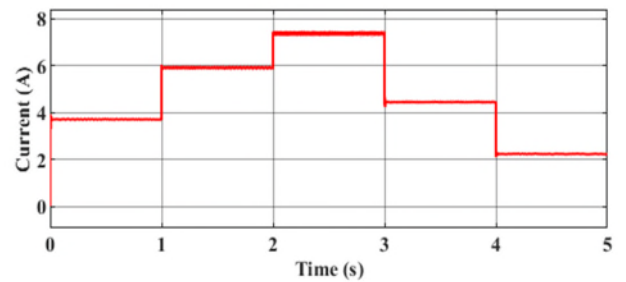


Figure. 8 Current of the PV

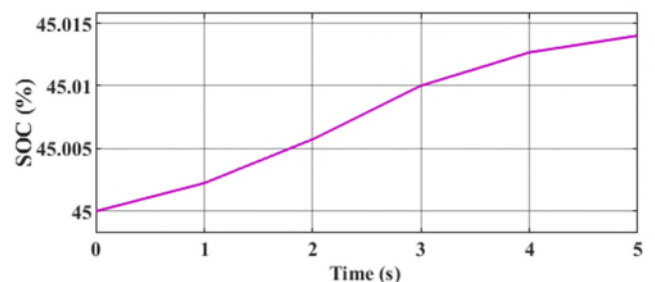


Figure. 9 Battery state of charge

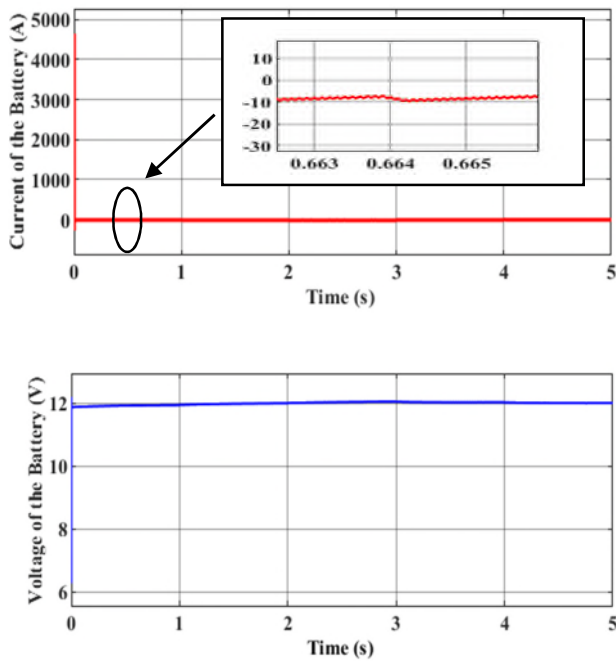


Figure. 10 output Charging Voltage & Current Of battery

The simulation is carried out using MATLAB/Simulink.

This work is carried out in Matlab/Simulink using the parameters listed in Table 2. An implementation of the proposed controller to verify its performance and robustness against climate change. In this section, we have considered that irradiation evolves according to the profile shown in figure 5, and that photovoltaic power corresponds perfectly to the maximum powers shown in figure 6. Figure 7 and 8 show the photovoltaic current and voltage, which also vary over the course of the previous profile. Figure 9 illustrates Battery state of charge, under the different irradiation values mentioned above.

Figure 10 shows the battery output voltage and current. Here, we focus on the variation times. It can be seen that both current and voltage change as a result of irradiation variation.

6. CONCLUSION

In this work, simulation results obtained with an implementation of the DISMC nonlinear controller as MPPT controller are presented for tracking MPP using a DC/DC boost converter for a system representing a maximum power of 212W. Simulation results are produced using Matlab/Simulink software. This algorithm (DISMC) does not require a reference rung to follow, but it does need to define the sliding surface. This method uses the incremental conductance technique as the sliding surface to track the PPM. The DISMC algorithm offers good performance and robustness through its testing under standard conditions and under conditions of abrupt climatic variation, and has the ability to reduce unwanted oscillations compared with other algorithms.

REFERENCES

[1] Byamakesh Nayak, Alivarani Mohapatra, Kanungo Barada Mohanty, Selection Criteria of DC-DC Converter

and Control Variable for MPPT of PV System Utilized in Heating and Cooking Applications, Cogent Engineering, 4, 1-16 (2017). 15.

- [2] Vinay Kumar, U.Salma, "Mathematical Modelling of a Solar Cell and its Performance Analysis under Uniform and Non-Uniform Insolation", International Journal of Engineering Research & Technology (IJERT), ISSN: 2278-0181, Vol. 6 Issue 12, December – 2017
- [3] Andújar, J. M., F. Segura, and T. Domínguez. 2016. "Study of a Renewable Energy Sources-based Smart Grid. Requirements, Targets and Solutions." 2016 3rd Conference on Power Engineering and Renewable Energy (ICPERE), Yogyakarta, 45–50.
- [4] Das P. Maximum power tracking based open circuit voltage method for PV system. In: International Conference on Advances in Energy Research (ICAER), Mumbai, India, 15–17 December 2015 published by Elsevier. p. 2–13.
- [5] Pradhan R, Subudhi B. Double integral sliding mode MPPT control of a photovoltaic system. IEEE Trans Control Syst Technol 2016;24(1):285–92.
- [6] Montoya DG, Andres C, Giral R. Improved design of sliding mode controllers based on the requirements of MPPT techniques. IEEE Trans Power Electron 2015:235–47.
- [7] Sowparnika GC, Sivalingam A, Thirumarimurugan M. Design and implementation of sliding mode control for boost converter using PV cell. Int Res J Emerg Trends Multidiscip (IRJETM) 2015;1(10):75–8.
- [8] Prabhakaran A, Mathew AS. Sliding mode MPPT based control for a solar photovoltaic system. Int Res J Eng Technol (IRJET) 2016;3(6):2600–4.
- [9] S. Zafar, Renewable Energy in Morocco, EcoMENA, 2019. (<https://www.ecomena.org/renewable-energy-inmorocco/>)
- [10] M.Kmaran, M.Mudassar, M.Rayyan Fazal, M.Usman, M.Bilal, R.Asghar, JKSU-ES, Implementation of improved Perturb & Observe MPPT technique with confined search space for standalone photovoltaic system, 32 (2020).
- [11] M.Shazly, A.S.Monstar, Reaserch Article, A comparative study of P&O and INC maximum power point tracking techniques for grid-connected PV systems, (2019)
- [12] Benhadouga S, Belkaid A, Colak I, Meddad M, & Eddiai A. Experimental Validation of The Sliding Mode Controller to Improve The Efficiency of The MPPT Solar System. In: 2021 10th International Conference on Renewable Energy Research and Application (ICRERA) (pp. 333-337). IEEE. (2021, September)
- [13]] Kchaou A, Naamane A, Koubaa Y, M'sirdi N. Second order sliding mode-based MPPT control for photovoltaic applications. Sol Energy 2017;155:758–69.
- [14]] Elazab OS, Debouza M, Hasanien HM, Muyeen SM, Al-Durra A. Salp swarm algorithm-based optimal control scheme for LVRT capability improvement of grid-connected photovoltaic power plants: design and experimental validation. IET Renew Power Gener 2020;14(4):591–9.
- [15] Fei J, Wang H, Fang Y. Novel neural network fractional-order sliding-mode control with application to active

- power filter. *IEEE Transactions on Systems, Man, and Cybernetics: Systems* 2021;52(6):3508–18.
- [16] Dragicevic T, Guerrero JM, Vasquez JC, Skrlec D. Supervisory control of an adaptive-droop regulated DC microgrid with battery management capability. *IEEE Trans Power Electron* 2014;29(2):695–706.
- [17] Byamakesh Nayak, Alivarani Mohapatra, Kanungo Barada Mohanty, Selection Criteria of DC-DC Converter and Control Variable for MPPT of PV System Utilized in Heating and Cooking Applications, *Cogent Engineering*, 4, 1-16 (2017). 15.



Three-Dimensional Fuzzy Logic Controller Applied to Rocket Target Traction

F. Bourourou¹, I.Habi², S.A.Tadjer^{3*}

¹ University M'hamed Bougara of Boumerdes, LREEI laboratory, f.bourourou@univ-boumerdes.dz

² University M'hamed Bougara of Boumerdes, LREEI laboratory, i.habi@univ-boumerdes.dz

³ University M'hamed Bougara of Boumerdes, LREEI laboratory, s.tadjer@univ-boumerdes.dz

Corresponding Author Email: f.bourourou@univ-boumerdes.dz

ABSTRACT

This paper deals with the three-dimensional fuzzy logic technique applications on target traction, where Rocket target traction is a complex process that requires precise control systems to ensure accurate targeting and trajectory. Traditional control systems have limitations in their ability to account for complex and nuanced conditions, leading to less accurate targeting and less efficient use of resources. Three-dimensional fuzzy logic is an advanced approach to control systems that allows for more precise and nuanced evaluations of conditions, leading to more accurate targeting and more efficient use of resources. In this article, we'll explore the application of three-dimensional fuzzy logic to rocket target traction, the benefits of this approach, and examples of its application in real-world scenarios using Matlab.

Received: 03/03/2023

Accepted: 29/07/2023

Published: 19/09/2023

Keywords:

Three-dimensional fuzzy logic Control, traction, simulation, programming, Matlab

1. INTRODUCTION

Rocket or Missile trajectory tracking is a critical technology used to guide missiles towards moving targets. The primary objective of missile trajectory tracking is to optimize (minimize) the distance between the missile and the target by calculating the optimal missile trajectory based on the current position and velocity of both the missile and the target. The key component of the guidance system is the tracking algorithm, and it plays a crucial role in achieving high-precision tracking of the target.

There are several types of guidance systems utilized for missile trajectory tracking, including radar, infrared, and laser guidance systems. Each system has its own strengths and limitations based on the flight conditions and target characteristics. Recent research has focused on developing advanced tracking algorithms to improve the precision of missile trajectory tracking. For example, researchers have investigated the use of machine learning techniques to enhance the accuracy of the tracking algorithm. In a recent study, convolutional neural networks were utilized to improve the accuracy of missile trajectory tracking [1].

In addition to developing advanced tracking algorithms, researchers have also explored the use of new sensors and trajectory calculation techniques to improve the precision of missiles. For instance, a recent combination of missiles. For instance, a recent combination of fuzzy logic controller and a linear

quadratic regulator to improve the guidance precision of the missile [2]. Another study proposed a new guidance algorithm based on a sliding mode control approach to improve the control accuracy of the missile [3].

Furthermore, researchers have also investigated the use of multi-sensor fusion techniques to enhance the tracking accuracy of missiles. For example, a recent study proposed a novel multi-sensor fusion algorithm based on a Kalman filter to improve the tracking accuracy of a missile guidance system [4].

So missile trajectory tracking is a critical technology for guiding missiles towards their targets. Advanced tracking algorithms, new sensors, and trajectory calculation techniques are being developed to improve the precision and range of missiles. Future research is expected to focus on developing more sophisticated tracking algorithms and novel guidance techniques to further improve the effectiveness of missile trajectory tracking. And for that this work is devoted to present a new Algorithm based on more developed control technique using the tree-dimensional fuzzy logic[5]-[9].

2. TREE-DIMENSIONAL FUZZY LOGIC

Fuzzy three-dimensional logic, also known as 3D fuzzy logic [10], is an extension of traditional fuzzy logic that allows for modelling three-dimensional systems using three-dimensional fuzzy sets.

Where Fuzzy logic was first introduced in the 1960 as a mathematical framework for dealing with uncertainty and imprecision in data. It was originally developed for

use in control systems, where precise, binary decisions were impractical. Fuzzy logic allowed for the creation of control systems that could make more flexible, nuanced decisions based on a range of input data.

In the early 1990s, researchers began to explore the use of fuzzy logic for modelling three-dimensional systems. One of the key challenges in this area was how to represent three-dimensional fuzzy sets mathematically. In 1992, Kaoru Hirota proposed a solution to this problem in a paper titled "Three-Dimensional Fuzzy Control".

Hirota's approach involved dividing a three-dimensional fuzzy set into a series of two-dimensional slices, each of which represented a different level of membership in the set. By representing the fuzzy set in this way, it was possible to perform calculations more efficiently and accurately.

2.1 Description of the Three-dimensional fuzzy logic

Three-dimensional fuzzy logic is an extension of traditional fuzzy logic that allows for the representation of fuzzy sets and membership functions in a three-dimensional space. This approach allows for more complex and nuanced evaluations of degrees of membership. Fuzzy logic is a mathematical approach that deals with uncertainty and imprecision by assigning degrees of truth rather than simply true or false. Traditional fuzzy logic represents fuzzy sets and membership functions in a two-dimensional space. In contrast, three-dimensional fuzzy logic represents fuzzy sets as volumes, called "3D membership functions." 3D membership functions are defined by mathematical equations that describe their shape and position in space. The fuzzy set is then determined by the intersection of several volumes. The fuzzy set of FLC and Type 2 FLC are represented in figure(1) below

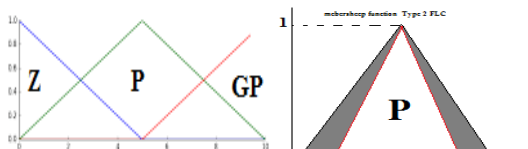


Figure.1 classical fuzzy logic set

Where fig 2 represent a tree dimensional fuzzy logic set

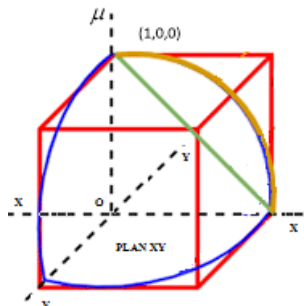


Figure.2 Tree dimensional fuzzy logic set

For the three dimensional axes X, Y, Z each axe has him three dimensional fuzzy set and the controller will use them all in the same time to locate the position of either

rocket and target and calculate the optimal estimated trajectory for the rocket.

2.2 Three-dimensional fuzzy logic advantages

The benefits of three-dimensional fuzzy logic include more accurate control and more efficient use of resources. Traditional control systems have limitations in their ability to account for complex and nuanced conditions, leading to less accurate control and less efficient use of resources. Three-dimensional fuzzy logic allows for more precise and nuanced evaluations of conditions, leading to more accurate control and more efficient use of resources but this need more complex algorithms and calculator more powerful to analyse the big data include in lesser time possible.

2.3 Three-dimensional fuzzy logic control principle

The most bases of the fuzzy logic controller are applied on three-dimensional fuzzy logic control but with three dimensional fuzzy set and the needed adaptation on fuzzification, inferences and defuzzification steps as shown on figure(3) below proposed by Volodymyr MORKUN and Olha KRAVCHENKO on 2021 in [11]

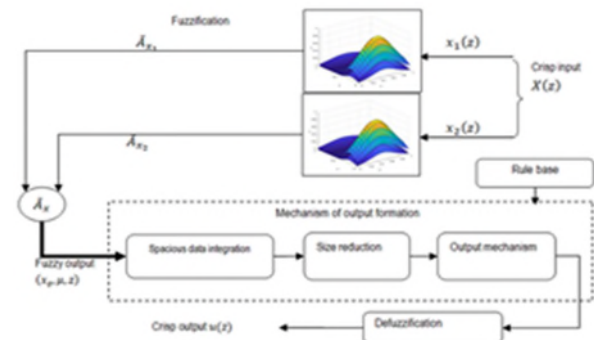


Figure.3 Three-dimensional fuzzy logic control principle [11]

Three-dimensional fuzzy logic is based on mathematical principles, including set theory, fuzzy set theory, and fuzzy logic. Set theory is used to define the universe of discourse, or the set of all possible values of a variable. Fuzzy set theory is used to define fuzzy sets, which are sets that have degrees of membership. Fuzzy logic is used to determine the degree of membership of a value in a fuzzy set.

Where the general basic control structure is represented on fig.4 describe the different parts of the fuzzy logic controller

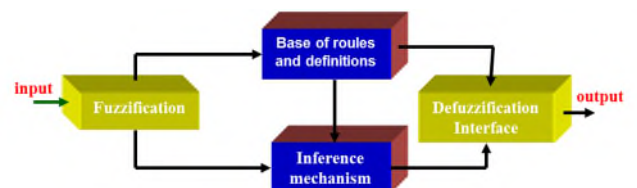


Figure.4 fuzzy logic controller structure

Also we can use the different bases rules of the traditional fuzzy logic with the three-dimensional fuzzy

logic controller with the consideration of the three dimensional member sheep set function.

3. THREE DIMENSIONAL FUZZY CONTROLER ALGORITHM

Three-dimensional fuzzy logic can be integrated into control systems using mathematical algorithms and programming languages. The algorithms are used to perform calculations and make decisions based on the input data and the fuzzy rule-based system. The programming languages are used to implement the algorithms and create the user interface for the control system.

The proposed controller algorithm steps are described on 7 points below:

Input and output variables definition

- 1) Member sheep function definition for each variable
- 2) Member sheep function plot
- 3) Control rules definition
- 4) Control rules aggregation
- 5) Global control rule plot
- 6) Command calculation
- 7) Command application to the system

For the input variable we have taken error on position and the error variation with the integral of the error as third input variable

Obtained results are represented in figures 5, 6 and 7

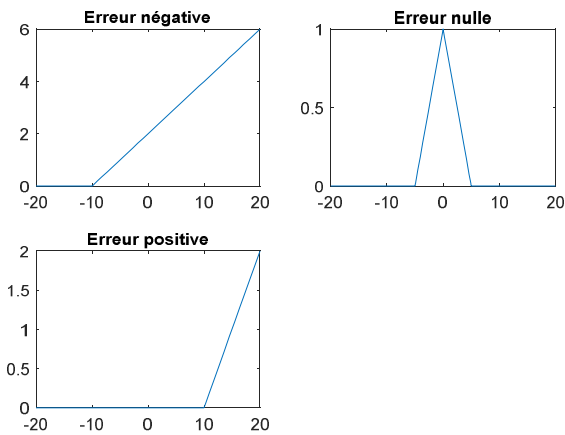


Figure.5 Three-dimensional fuzzy logic control input set "error"

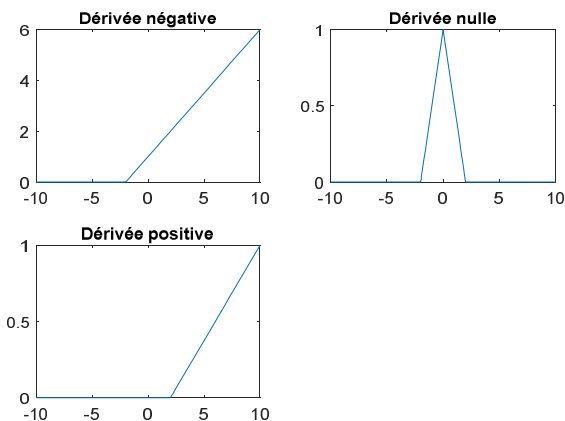


Figure.6 Three-dimensional fuzzy logic control input set "de"

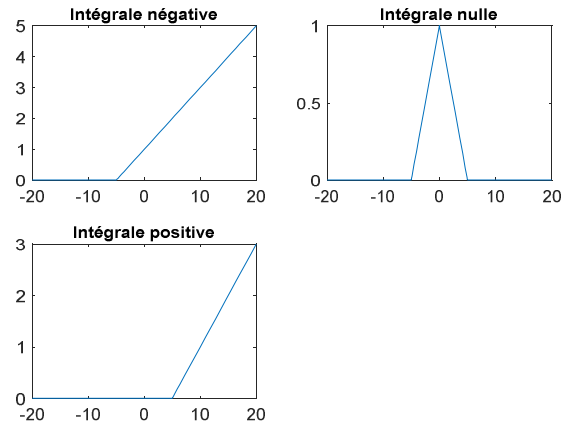


Figure.7 Three-dimensional fuzzy logic control input set "error integral"

Where the command output is represented by figure.8

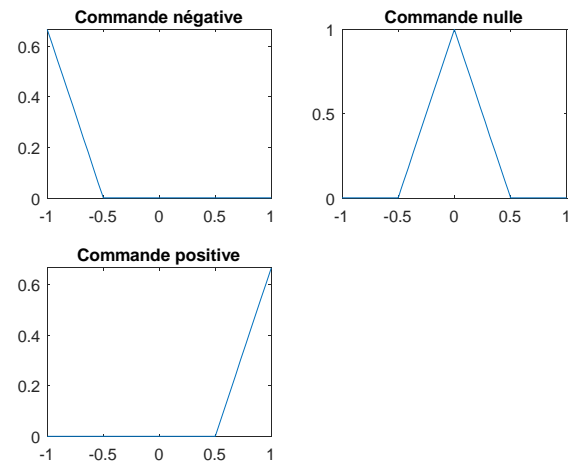


Figure.8 Three-dimensional fuzzy logic control output set "u"

And the control rules are represented on figure.9

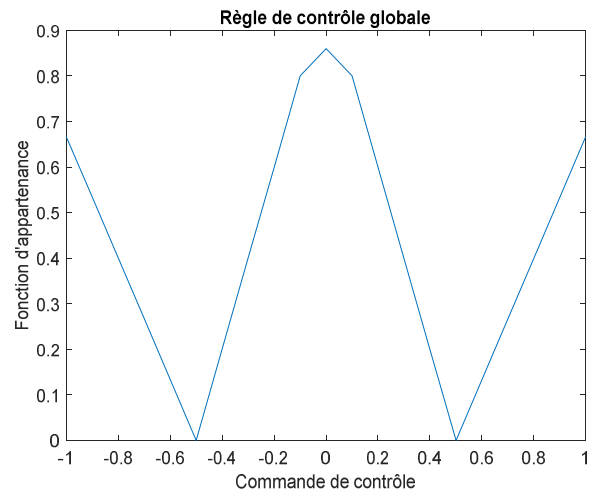


Figure.9 Three-dimensional fuzzy logic global control rules

4. THREE-DIMENSIONAL FUZZY LOGIC APPLIED TO ROCKET TARGET TRACTION

Three-dimensional fuzzy logic can be implemented in rocket target traction by creating 3D membership functions for each variable that affects the trajectory of the rocket. These variables may include altitude, velocity, trajectory, wind speed, and direction. The 3D membership functions are then combined to create a fuzzy rule-based system that determines the optimal thrust, angle, and direction of the rocket.

As example of the application of three-dimensional fuzzy logic to rocket target traction is the landing of the Mars Rover on the surface of Mars. The landing process involves multiple stages, including entry, descent, and landing. During the descent stage, the rocket engine must be controlled to ensure a safe and accurate landing. Three-dimensional fuzzy logic can be used to regulate the thrust of the rocket engine based on observed measurements, such as altitude, velocity, and trajectory. It can also be used to adjust the angle and direction of the rocket in response to changing conditions, such as wind speed and direction.

The Mars Pathfinder mission, launched in 1996, utilized fuzzy logic to control the descent of the spacecraft onto the surface of Mars. The fuzzy logic system was used to adjust the thrusters of the spacecraft to keep it on course as it descended towards the surface. The system was able to adjust to unexpected wind gusts and keep the spacecraft on target, resulting in a successful landing.

5. CONCLUSIONS

Three-dimensional fuzzy logic is an advanced approach to control systems that allows for more precise and nuanced evaluations of conditions, leading to more accurate targeting and more efficient use of resources. It can be applied in many fields, including rocket target traction, where it can be used to regulate the thrust, angle, and direction of the rocket engine based on observed measurements. The mathematical integration of three-dimensional fuzzy logic in control systems is based on set theory, fuzzy set theory, and fuzzy logic, and can be implemented using mathematical algorithms and programming languages. With its ability to handle complex and nuanced conditions, three-dimensional fuzzy logic has the potential to revolutionize the field of control systems and improve the accuracy and efficiency of many processes.

Acknowledgment

My Acknowledgment is directed to the LREEI laboratory director, professor I.Habi in FHC on the university of M'Hamed Bougara of Boumerdes.

REFERENCES

- [1] Cao, Y, Liu, Y, Wang, F, & Zhang, L, "A Convolutional Neural Network Based Method for Missile Trajectory Tracking". *IEEE Transactions on Aerospace and Electronic Systems*, 56(6), 4374-438, 2020.
- [2] Chen, Y, Xu, Y, & Wang, H, "Fuzzy Linear Quadratic Guidance Law Design for Missile Trajectory Tracking". *Applied Sciences*, 11(2), 820, 2021.
- [3] Li, Y, Zhang, Y, Li, Z, & Li, X, "Sliding mode control-based guidance law and control for missile trajectory tracking", *Aerospace Science and Technology*, 104989, 2020.
- [4] Yang, L, Zhang, S, Liu, X., & Li, Y, "Novel Multi-sensor Fusion Algorithm for Missile Guidance System Based on Kalman Filter", *IEEE Sensors Journal*, 21(4), 4258-4268., 2021.
- [5] Bezdek, J. C, & Pal, S. K, "Fuzzy Models for Pattern Recognition". *IEEE Press*, 1992.
- [6] Gu, Y, & Wang, L. X, "Fuzzy Control and Modeling: Analytical Foundations and Applications". *IEEE Press*, 2002.
- [7] Li, H, Wang, D, & Liang, Y, "Three-dimensional fuzzy control method for voltage regulation in photovoltaic stations", *Journal of Renewable Energy*, 32(11), 1874-1884, 2007.
- [8] Liu, J, & Huang, X, "Three-dimensional fuzzy control of voltage regulation in photovoltaic stations based on genetic algorithm", *International Journal of Control and Automation*, 11(1), 45-54, 2018.
- [9] Yang, Y., & Liu, C, "Three-dimensional fuzzy control of voltage regulation in photovoltaic stations based on improved particle swarm optimization algorithm", *International Journal of Control and Automation*, 10(12), 95-104, 2017.
- [10] Chen, Y, & Li, Y, "A Three-Dimensional Fuzzy Control Strategy for Permanent Magnet Synchronous Generator Wind Turbine Systems", *IEEE Transactions on Power Electronics*, 34(10), 10059-10072, 2019.
- [11] Volodymyr Morkun, Olha Kravchenko, "Three-Dimensional Fuzzy Control Of Ultrasonic Cleaning", *Acta Mechanica Et Automatica*, Vol.15 No.3, 2021.